



1 **Argon offline-AMS source apportionment of organic**  
2 **aerosol over yearly cycles for an urban, rural and marine**  
3 **site in Northern Europe**

4  
5 **C. Bozzetti<sup>1</sup>, Y. Sosedova<sup>1</sup>, M. Xiao<sup>1</sup>, K. R. Daellenbach<sup>1</sup>, V. Ulevicius<sup>2</sup>, V.**  
6 **Dudoitis<sup>2</sup>, G. Mordas<sup>2</sup>, S. Byčenkienė<sup>2</sup>, K. Plauškaitė<sup>2</sup>, A. Vlachou<sup>1</sup>, B. Golly<sup>3</sup>, B.**  
7 **Chazeau<sup>1</sup>, J.-L. Besombes<sup>4</sup>, U. Baltensperger<sup>1</sup>, J.-L. Jaffrezo<sup>3</sup>, J. G. Slowik<sup>1</sup>, El**  
8 **Haddad<sup>1</sup>, I., and A. S. H. Prévôt<sup>1</sup>**

9 [1] {Laboratory of Atmospheric Chemistry, Paul Scherrer Institute (PSI), 5232 Villigen-PSI,  
10 Switzerland}

11 [2] {Department of Environmental Research, SRI Center for Physical Sciences and  
12 Technology, LT-02300 Vilnius, Lithuania}

13 [3] {Université Grenoble Alpes, CNRS, LGGE, 38000 Grenoble, France}

14 [4] {Université Savoie Mont-Blanc, LCME, F-73000 Chambéry, France}

15

16 Correspondence to: A. S. H. Prévôt ([andre.prevot@psi.ch](mailto:andre.prevot@psi.ch)); I. El Haddad ([imad.el-](mailto:imad.el-haddad@psi.ch)  
17 [haddad@psi.ch](mailto:haddad@psi.ch))

18

19 **Abstract**

20 The widespread use of Aerodyne aerosol mass spectrometers (AMS) has greatly improved  
21 real-time organic aerosol (OA) monitoring, providing mass spectra that contain sufficient  
22 information for source apportionment. However, AMS field deployments remain expensive  
23 and demanding, limiting the acquisition of long-term datasets at many sampling sites. The  
24 offline application of aerosol mass spectrometry entailing the analysis of nebulized water  
25 extracted filter samples (offline-AMS) increases the spatial coverage accessible to AMS  
26 measurements, being filters routinely collected at many stations worldwide.

27 PM<sub>1</sub> (particulate matter with an aerodynamic diameter <1 μm) filter samples were collected  
28 during an entire year in Lithuania at three different locations representative of three typical



1 environments of the South-East Baltic region: Vilnius (urban background), Rūgštelėškis (rural  
2 terrestrial), and Preila (rural coastal). Aqueous filter extracts were nebulized in Ar, yielding  
3 the first AMS measurements of water-soluble atmospheric organic aerosol (WSOA) without  
4 interference from air fragments. This enables direct measurement of the  $\text{CO}^+$  fragment  
5 contribution, whose intensity is typically assumed to be equal to that of  $\text{CO}_2^+$ . Offline-AMS  
6 spectra reveal that the water soluble  $\text{CO}_2^+:\text{CO}^+$  ratio not only shows values systematically  $<1$   
7 but is also dependent on season, with lower values in winter than in summer.

8 AMS WSOA spectra were analyzed using positive matrix factorization (PMF), yielding 5  
9 factors: traffic exhaust OA (TEOA), biomass burning OA (BBOA), local OA (LOA)  
10 contributing significantly only in Vilnius, and two oxygenated OA (OOA) factors  
11 distinguished by seasonal variability. AMS-PMF source apportionment results were  
12 consistent with those obtained from PMF applied to marker concentrations (i.e. major  
13 inorganic ions, OC/EC, and organic markers including polycyclic aromatic hydrocarbons and  
14 their derivatives, hopanes, long-chain alkanes, monosaccharides, anhydrous sugars, and lignin  
15 fragmentation products). OA was the largest fraction of  $\text{PM}_{10}$  and was dominated by BBOA  
16 during winter with an average concentration of  $2 \mu\text{g m}^{-3}$  (53% of OA), while summer-OOA  
17 (S-OOA), probably related to biogenic emissions was the prevalent OA source during  
18 summer with an average concentration of  $1.2 \mu\text{g m}^{-3}$  (45% of OM).

19 PMF ascribed a large part of the  $\text{CO}^+$  explained variability (97%) to the OOA and BBOA  
20 factors. Accordingly we discuss a new  $\text{CO}^+$  parameterization as a function of  $\text{CO}_2^+$ , and  
21  $\text{C}_2\text{H}_4\text{O}_2^+$  fragments, which were selected to describe the variability of the OOA and BBOA  
22 factors.

## 23 1 Introduction

24 Atmospheric aerosols affect climate (Lohmann et al., 2004, Schwarze et al., 2006), human  
25 health (Dockery et al., 2005, Laden et al., 2000), and ecosystems on a global scale.  
26 Quantification and characterization of the main aerosol sources are crucial for the  
27 development of effective mitigation strategies. The Aerodyne aerosol mass spectrometer  
28 (AMS, Canagaratna et al., 2007) and aerosol chemical speciation monitor (ACSM, Ng et al.,  
29 2011, Fröhlich et al., 2013) have greatly improved air quality monitoring by providing real-  
30 time measurements of the non-refractory (NR) submicron aerosol ( $\text{PM}_{10}$ ) components.  
31 Analysis of organic mass spectra using positive matrix factorization (PMF, Paatero, 1997;  
32 Paatero and Tapper, 1994) has enabled the quantitative separation of OA factors, which can



1 be subsequently related to major aerosol sources and formation processes (e.g. Lanz et al.,  
2 2007; Lanz et al., 2010; Zhang et al., 2011; Ulbrich et al., 2009; Elser et al., 2016 a). Despite  
3 its numerous advantages, AMS field deployment remains expensive and demanding, and  
4 therefore most of the studies are typically restricted to short-time periods and a single (or few)  
5 sampling site(s). The limited amount of long-term datasets suitable for OA source  
6 apportionment severely limits model testing and validation (Aksoyoglu et al., 2011;  
7 Aksoyoglu et al., 2014; Baklanov et al., 2014), as well as for the development of appropriate  
8 pollution mitigation strategies. AMS analysis of aerosol filter samples (Lee et al., 2011; Sun  
9 et al., 2011; Mihara and Mochida, 2011; Daellenbach et al., 2016), which are routinely  
10 collected at many stations worldwide, broadens the temporal and spatial scales available for  
11 AMS measurements.

12 In this study we present the application of the offline-AMS methodology described by  
13 Daellenbach et al. (2016) to yearly cycles of filter samples collected in parallel at three  
14 different locations in Lithuania between September 2013 and August 2014. The methodology  
15 consists of water extraction of filter samples, followed by nebulization of the liquid extracts,  
16 and subsequent measurement of the generated aerosol by high-resolution time-of-flight AMS  
17 (HR-ToF AMS). In this work, organic aerosol water extracts were nebulized in Ar, permitting  
18 direct measurement of the  $\text{CO}^+$  ion (Fig. S1), which is typically not directly quantified in  
19 AMS data analysis due to interference with  $\text{N}_2^+$ , but is instead estimated as being equal to  
20  $\text{CO}_2^+$  (Aiken et al., 2008). Direct measurement of  $\text{CO}_2^+$  better captures the variability in the  
21 total OA mass and its elemental composition as well as potentially improving source  
22 apportionment of ambient aerosol. Aerosol elemental ratios and oxidation state are of  
23 particular relevance as they provide important constraints for understanding aerosol sources,  
24 processes, and for the development of predictive aerosol models (Canagaratna et al., 2015).

25 Aerosol composition in the south-east Baltic region has so far received little attention. To our  
26 knowledge the only investigation of OA sources in this area was during a five-day period of  
27 intense land clearing activity occurring in the neighboring Russian enclave of Kaliningrad  
28 (Ulevicius et al., 2015; Dudoitis et al., 2016), in which transported biomass burning emissions  
29 dominated the aerosol loading. OA source contributions under less extreme conditions remain  
30 unstudied, with the most relevant measurements performed in Estonia with a mobile lab  
31 during March 2014 at two different locations (Elser et al., 2016b). On-road measurements  
32 revealed large traffic contributions with an increase of 20% from rural to urban environments.



1 Also, residential biomass burning (BB) and oxygenated OA (OOA) contributions were found  
2 to be substantial.

3 In this study we present a complete source apportionment of the submicron OA fraction  
4 following the methodology described by Daellenbach et al. (2016) in order to quantify and  
5 characterize the main OA sources affecting the Lithuanian air quality. The three sampling  
6 stations were situated in the Vilnius suburb (urban background), Preila (rural coastal  
7 background), and Rūgštelėškis (rural terrestrial background), covering a wide geographical  
8 domain and providing a good overview of the most typical Lithuanian and south-eastern  
9 Baltic air quality conditions and environments. PMF analysis of offline-AMS measurements  
10 are compared with the results reported by Ulevicius et al. (2015) and with PMF analysis of  
11 chemical marker measurements obtained from the same filter samples.

## 12 **2 Sampling and offline measurements**

### 13 **2.1 Site description and sample collection**

14 We collected 24-h integrated PM<sub>1</sub> filter samples at 3 different stations in Lithuania from 30  
15 September 2013 to 2 September 2014 using 3 High-Volume samplers (Digital DHA80, and  
16 DH-77) operating at 500 L min<sup>-1</sup>. The particulate matter was collected on 150-mm diameter  
17 quartz fiber filters (Pallflex Tissuquartz 2500QAT-UP / pure quartz, no binder) pre-baked at  
18 800°C for 8 h. Filter samples were wrapped in pre-baked aluminum foils (400°C for 6 h),  
19 sealed in polyethylene bags and stored at -20°C after exposure. Field blanks were collected  
20 and stored following the same procedure.

21 Sampling was conducted at urban (Vilnius), rural terrestrial (Rūgštelėškis) and rural coastal  
22 (Preila) monitoring sites (Fig. 1). The rural terrestrial site of Rūgštelėškis serves as a baseline  
23 against which urban-specific sources in the major population center of Vilnius can be  
24 compared. The rural coastal site of Preila provides an opportunity to distinguish terrestrial and  
25 marine sources.

26 The sampling station in Vilnius is located at the Center for Physical Sciences and Technology  
27 campus (54°38' N, 25°10' E, 165 m a.s.l.) 12 km southwest of the city center (population:  
28 535000) and is classified as an urban background site. The site is relatively far from busy  
29 roads, and surrounded by forests to the north/northeast, and by a residential zone to the  
30 south/east. It is ca. 350 km distant from the Baltic coast, and 98 km from the Rūgštelėškis  
31 station (Fig. 1).



1 The station in Preila (55°55' N, 21°04' E, 5 m a.s.l.) is a representative rural coastal  
2 background site, situated in the Curonian Spit National Park on the isthmus separating the  
3 Baltic Sea from the Curonian Lagoon. The monitoring station is located <100 m from the  
4 Baltic shore. The closest populated area is the village of Preila (population: 200 inhabitants),  
5 located 2 km to the south.

6 The rural terrestrial station of Rūgštelėškis (55°26' N and 26°04' E, 170 m a.s.l.) is located in  
7 the eastern part of Lithuania, about 350 km from the Baltic Sea. The site is surrounded by  
8 forest and borders the Utenas Lake in the southwest. The nearest residential areas are  
9 Tauragnai, Utena (12 km and 26 km west of the station, population: 32000 inhabitants) and  
10 Ignalina (17 km southeast of the station, population: 6000 inhabitants).

## 11 2.2 Offline-AMS analysis

12 The term *offline-AMS* will be used herein to refer to the methodology described by  
13 Daellenbach et al. (2016) and summarized below. For each analyzed filter sample, four 16-  
14 mm diameter filter punches were subjected to ultrasonic extraction in 15 mL of ultrapure  
15 water (18.2 MΩ cm at 25°C, total organic carbon (TOC) < 3 ppb) for 20 min at 30°C.

16 The choice of water instead of an organic solvent is motivated by two arguments:

- 17 - Water yields the lowest background and hence the highest signal to noise compared to  
18 other highly pure solvents (including methanol, dichloromethane and ethyl acetate).
- 19 - In contrast to the water extraction, the use of organic solvents precludes the  
20 quantification of the organic content in the extracts (e.g. by using a total OC analyzer),  
21 which in turn prevents a quantitative source apportionment.

22 Liquid extracts were then filtered and atomized in Ar (≥99,998 % Vol. abs., Carbagas, CH-  
23 3073 Gümligen, Switzerland) using an Apex Q nebulizer (Elemental Scientific Inc., Omaha  
24 NE 68131 USA) operating at 60°C. The resulting aerosol was then dried by passing through a  
25 Nafion drier (Perma Pure, Toms River NJ 08755 USA), and subsequently analyzed by a HR-  
26 ToF-AMS. 12 mass spectra per filter sample were collected (AMS V-mode,  $m/z$  12-232, 30 s  
27 collection time per spectrum). A measurement blank was recorded before and after each  
28 sample by nebulizing ultrapure water for 12 minutes. Field blanks were measured following  
29 the same extraction procedure as the collected filter samples, yielding a signal not statistically  
30 different from that of nebulized milliQ water. Finally we registered the AMS fragmentation



1 spectrum of pure gaseous CO<sub>2</sub> (≥99,7 % Vol, Carbagas, CH-3073 Gümligen, Switzerland), in  
2 order to derive its CO<sub>2</sub><sup>+</sup>:CO<sup>+</sup> ratio.

3 Offline-AMS analysis was performed on 177 filter samples in order to determine the bulk  
4 water-soluble organic matter (WSOM) mass spectral fingerprints. In total, 63 filters from  
5 Rūgšteliškis, 42 from Vilnius, and 71 from Preila were measured in Ar. The reader is referred  
6 to DeCarlo et al. (2006) for a thorough description of the AMS operating principles and  
7 calibration procedures.

8 HR-ToF-AMS analysis software SQUIRREL (SeQUential Igor data RetRiEvaL, D. Sueper,  
9 University of Colorado, Boulder, CO, USA) v.1.53G and PIKA (Peak Integration by Key  
10 Analysis) v.1.11L for IGOR Pro software package (Wavemetrics, Inc., Portland, OR, USA)  
11 were utilized to process and analyze the AMS data. HR analysis of the AMS mass spectra was  
12 performed in the *m/z* range 12-115.

### 13 **2.3 Supporting measurements**

14 Additional offline analyses were carried out in order to validate and corroborate the offline-  
15 AMS source apportionment results. This supporting dataset was also used as input for PM<sub>1</sub>  
16 source apportionment as discussed below. The complete list of the measurements performed  
17 can be found in Table 1 and Table S1. Briefly, major ions were measured by ion  
18 chromatography (IC; Jaffrezo et al., 1998); elemental and organic carbon (EC, OC) were  
19 quantified by thermal optical transmittance following the EUSAAR2 protocol (Cavalli et al.,  
20 2010); water-soluble OC (WSOC) was measured by water extraction followed by catalytic  
21 oxidation and non-dispersive infrared detection of CO<sub>2</sub> using a total organic carbon analyzer  
22 (Jaffrezo et al., 2005). Organic markers were determined by gas chromatography-mass  
23 spectrometry (GC-MS; Golly et al., 2015); high performance liquid chromatography (HPLC)  
24 associated with a fluorescence detector (LC 240 Perkin Elmer) and HPLC-pulsed  
25 amperometric detection (PAD; Waked et al., 2014) for 67 composite samples. Composites  
26 were created merging two consecutive filter samples, but no measurements are available for  
27 Vilnius during summer. Measurements included 18 polycyclic aromatic hydrocarbons  
28 (PAHs), alkanes (C21-C40), 10 hopanes, 13 methoxyphenols, 13 methyl-PAHs (Me-PAHs), 6  
29 sulfur-containing-PAHs (S-PAHs), 3 monosaccharide anhydrides, and 4 monosaccharides  
30 (including glucose, mannose, arabitol, and mannitol). In this work ion concentrations always  
31 refer to the IC measurements.



- 1 Table 1. Overview of supporting measurements. A complete list of measured compounds can  
 2 be found in table S1.

Analytical Method	Measured compounds	Filters measured
IC (Jaffrezo et al., 1998)	Ions	All
	EC/OC	
Thermal optical transmittance using Sunset Lab Analyzer (Birch and Cary, 1996) using EUSAAR2 protocol (Cavalli et al., 2010)		All
TOC analyzer using persulphate oxidation at 100°C of the OM, followed by CO <sub>2</sub> quantification with a non-dispersive infrared spectrophotometer (Jaffrezo et al., 1998)	WSOC	All
HPLC associated with fluorescence detector (LC 240 Perkin Elmer) (Golly et al., 2015, Besombes et al., 2001)	PAHs (table S1)	67 composite samples
GC-MS (with and without derivatization step) (Golly et al., 2015)	S-PAHs, Me-PAHs, alkanes, hopanes, methoxyphenols, others	67 composite samples
HPLC-PAD, (Waked et al., 2014)	Anhydrous sugars, sugars alcohols, monosaccharides	67 composite samples
Chemiluminescence (Environnement S.A., Model AC31M)	NO <sub>x</sub>	Online (Vilnius only)



1 In the following, subscripts *avg*, and *med* will denote average and median values,  
2 respectively.

### 3 **3 Source apportionment**

4 Positive matrix factorization (PMF, Paatero and Tapper, 1994) is a bilinear statistical model  
5 used to describe the variability of a multivariate dataset as the linear combination of a set of  
6 constant factor profiles and their corresponding time series, as shown in Eq. (1):

$$7 \quad x_{i,j} = \sum_{z=1}^p (g_{i,z} \cdot f_{z,j}) + e_{i,j} \quad (1)$$

8 Here *x*, *g*, *f*, and *e* denote elements of data, factor time series, factor profiles and residual  
9 matrices, respectively, while subscripts *i,j* and *z* are indices for time, measured variables, and  
10 factor number. The value *p* represents the total number of factors chosen for the PMF  
11 solution. The PMF algorithm iteratively solves Eq. (1) by minimizing the objective function  
12 *Q*, defined in Eq. (2) Only non-negative *g<sub>i,z</sub>* and *f<sub>z,j</sub>* values are permitted:

$$13 \quad Q = \sum_i \sum_j \left( \frac{e_{i,j}}{s_{i,j}} \right)^2 \quad (2)$$

14 Here the *s<sub>i,j</sub>* elements represent entries in the input error matrix.

15 In this work the PMF algorithm was run in the robust mode in order to dynamically  
16 downweigh the outliers. The PMF algorithm was solved using the multilinear engine-2 (ME-  
17 2) solver (Paatero, 1999), which enables an efficient exploration of the solution space by *a*  
18 *priori* constraining the *g<sub>i,z</sub>* or *f<sub>z,j</sub>* elements within a certain variability defined by the scalar *a*  
19 ( $0 \leq a \leq 1$ ) such that the modelled *g<sub>i,z</sub>*' and *f<sub>z,j</sub>*' satisfy Eq. (3):

$$20 \quad \frac{(1-a)f_{z,n}}{(1+a)f_{z,n}} \leq \frac{f_{z,n'}}{f_{z,m'}} \leq \frac{(1+a)f_{z,n}}{(1-a)f_{z,m}} \quad (3)$$

21 Here *n* and *m* are any two arbitrary columns (variables) in the normalized F matrix. The  
22 Source Finder toolkit (SoFi, Canonaco et al., 2013, v.4.9) for Igor Pro software package  
23 (Wavemetrics, Inc., Portland, OR, USA) was used to configure the ME-2 model and for post-  
24 analysis. PMF analysis was applied to two complementary datasets: (1) organic mass spectra  
25 from offline-AMS measurements for the apportionment of OM sources and (2) molecular  
26 markers for the apportionment of the measured PM<sub>1</sub> mass. These two analyses are discussed  
27 separately below.

28





### 1 3.1 Offline-AMS PMF

2 In the following section we describe the offline-AMS source apportionment implementation,  
3 optimization and uncertainty assessment. Briefly, we selected the number of PMF factors  
4 based on residual analyses and solution interpretability; subsequently we explored the  
5 rotational uncertainty of our source apportionment model and discarded suboptimal solutions  
6 providing insufficient correlation of factor time series with external tracers. The offline-AMS  
7 source apportionment returns the water soluble PMF factor concentrations. Daellenbach et al.  
8 (2016) determined factor specific recoveries (including the extraction efficiencies), by  
9 comparing offline-AMS and online-ACSM source apportionments. Applying these recoveries  
10 enabled scaling the water soluble factor concentrations to the corresponding bulk OA  
11 concentrations. A sensitivity analysis of these recoveries was reported in Section 3.1.3, and  
12 the corresponding uncertainty was propagated to the source apportionment results.

13 A second selection step was carried out on the rescaled solutions as described in section 3.1.3.  
14 The offline-AMS source apportionment results presented in this study represent the average  
15 of the retained rescaled PMF solutions, while their variability represents our best estimate of  
16 the source apportionment uncertainty.

#### 17 3.1.1 Inputs

18 The offline-AMS input matrices include in total 177 filter samples (62 filters from  
19 Rūgšteliškis, 42 from Vilnius, and 73 from Preila). Each filter sample was represented on  
20 average by 12 mass spectral repetitions to explore the effect of AMS and nebulizer stability  
21 on PMF outputs. A corresponding measurement blank was subtracted from each mass  
22 spectrum. The input PMF matrices included 269 organic fragments fitted in the mass range  
23 (12-115). The input error  $s_{i,j}$  elements include the blank variability ( $\sigma_{i,j}$ ) and the uncertainty  
24 related to ion counting statistic and ion-to-ion signal variability at the detector ( $\delta_{i,j}$ , Allan et  
25 al., 2003; Ulbrich et al., 2009):

$$26 \quad s_{i,j} = \sqrt{\delta_{i,j}^2 + \sigma_{i,j}^2} \quad (4)$$

27 We applied a minimum error to the  $s_{i,j}$  matrix elements according to Ulbrich et al. (2009), and  
28 a down-weighting factor of 3 to all fragments with an average signal to noise lower than 2  
29 (Ulbrich et al., 2009). Input data and error matrices were rescaled such that the sum of each  
30 row is equal to the estimated WSOM concentration, which is calculated as the product of the



1 measured WSOC multiplied by the  $OM:OC_i$  ratios determined from the offline-AMS PMF  
2 results.

### 3 3.1.2 Overview of retrieved factors and estimate of traffic exhaust OA (TEOA)

4 We used a 4-factor solution to represent the variability of the input data. The 4 separated OA  
5 factors included the following:

6 1/ a biomass burning OA (BBOA) factor highly correlated with levoglucosan originating from  
7 cellulose pyrolysis;

8 2/ a local OA (LOA) factor explaining a large fraction of N-containing fragments variability  
9 and contributing mostly in Vilnius during summer and spring;

10 3/ a background oxygenated-OA (B-OOA) factor showing relatively stable contributions at all  
11 seasons;

12 4/ a summer-OOA (S-OOA) factor showing increasing concentrations with the average daily  
13 temperature.

14 If the number of factors is decreased to 3, a mixed BBOA/B-OOA factor is retrieved, and  
15 significant structure appears in the residuals during winter (Fig. S2, S3, S4). Increasing the  
16 number of factors to 5 and 6, leads to a splitting of OOA factors that cannot be interpreted in  
17 terms of specific aerosol sources/processes (Fig. S2, S3). The further separated OOA factor in  
18 the 5-factor solution possibly derived from the splitting of B-OOA; in fact the sum of the  
19 newly separated OOA and B-OOA in the 5-factor solution correlated well with the B-OOA  
20 time series from the 4-factor solution ( $R = 0.93$ ). Overall, a clear structure removal in the  
21 residual time-series was observed until a number of factors equal to 4 (Fig. S4, S5).

22 We also explored a 5-factor solution in which a hydrocarbon-like OA (HOA) profile from  
23 Mohr et al. (2012) to estimate the TEOA contribution. However, the water-soluble TEOA  
24 (WSTEOA) contribution to WSOM was estimated as  $0.2\%_{\text{avg}}$  (section 3.1.4), likely too small  
25 for PMF to resolve. We performed 100 PMF runs by randomly varying the HOA  $\alpha$ -value. The  
26 obtained results showed a low TEOA correlation with hopanes ( $R_{\text{max}} = 0.25$ ,  $R_{\text{min}} = -0.15$ )  
27 with 45% of the PMF runs associated with negative Pearson correlation coefficients,  
28 supporting the hypothesis that this factor has too small a contribution to be resolved.  
29 Therefore, we selected the 4-factor solution as our best representation of the data, while



1 TEOA was instead estimated by a chemical mass balance (CMB) approach and not based on  
2 AMS mass spectral features.

3 TEOA concentrations are estimated using a CMB approach that assumes hopanes, present in  
4 lubricant oils engines, (Subramanian et al., 2006) to be unique tracers for traffic. However,  
5 hopanes can also be emitted upon combustion of different types of fossil fuel, in particular by  
6 coal combustion (Rutter et al., 2009), therefore the traffic contribution estimated here,  
7 although very small (as discussed in the result section) should be considered as an upper  
8 estimate. Still, the EC/hopanes ratio determined in this work ( $900 \pm 100$ ) is consistent with  
9 EC/hopanes for TE ( $1400 \pm 900$ : He et al., 2006; He et al., 2008; El Haddad et al., 2009; Fraser  
10 et al., 1998) and not with the coal EC/hopanes from literature profiles ( $300 \pm 200$ : Huang et al.,  
11 2014; supplementary information (SI)). To assess the traffic exhaust OC (TEOC) contribution  
12 we used the sum of the four most abundant hopanes (17a(H),21b(H)-norhopane,  
13 17a(H),21b(H)-hopane, 22S,17a(H),21b(H)-homohopane, and 22R,17a(H),21b(H)-  
14 homohopane (hopanes<sub>sum</sub>)). The TEOC contribution was estimated from the average  
15 hopanes<sub>sum</sub>/TEOC ratio ( $0.0012 \pm 0.0005$ ) from tunnel measurements reported by He et al.  
16 (2006), He et al. (2008), El Haddad et al. (2009), and Fraser et al. (1998), where the four  
17 aforementioned hopanes were also the most abundant. In order to rescale TEOC to the total  
18 TEOA concentration we assumed an OM:OC<sub>TEOA</sub> ratio of  $1.2 \pm 0.1$  (Aiken et al., 2008, Mohr  
19 et al., 2012, Docherty et al., 2011, Setyan et al., 2012). The uncertainty of the estimated  
20 TEOA concentration was assessed by propagating the uncertainties relative to the  
21 OM:OC<sub>TEOA</sub> ratio (8.3%), the hopanes<sub>sum</sub>/TEOC ratio (41.7%), the hopane measurement  
22 repeatability (11.5%), and detection limits ( $7 \text{ pg m}^{-3}$ ).

23

### 24 3.1.3. Source apportionment uncertainty

25 A common issue in PMF is the exploration of the rotational ambiguity, here addressed by  
26 performing 100 PMF runs initiated using different input matrices. We adopted a bootstrap  
27 approach (Davison and Hinkley, 1997) to generate the new input data and error matrices  
28 (Brown et al., 2015). Briefly, the bootstrap algorithm generates new input matrices by  
29 randomly resampling mass spectra from the original input matrices. As already mentioned,  
30 the input matrices contained ca. 12 mass spectral repetitions per filter sample; therefore the  
31 bootstrap approach was implemented in order to resample random filter sample mass spectra  
32 together with the corresponding measurement repetitions. Each newly generated PMF input



1 matrix had a total number of samples equal to the original matrices (177 samples), although  
 2 some of the original 177 filter samples are represented several times, while others are not  
 3 represented at all. Overall we resampled on average  $63 \pm 2\%$  of the filter samples per bootstrap  
 4 run. The generated data matrices were finally perturbed by varying each  $x_{i,j}$  element within  
 5 twice the corresponding uncertainty ( $s_{i,j}$ ) assuming a normal distribution of the errors.  
 6 Solutions were selected and retained according to three acceptance criteria. Solutions were  
 7 selected and retained according to three acceptance criteria based on PMF factor correlations  
 8 with corresponding tracers: BBOA vs. levoglucosan, B-OOA vs.  $\text{NH}_4^+$ , and S-OOA vs.  
 9 average daily temperature. In order to discard suboptimal PMF runs, we only retained  
 10 solutions associated with positive Pearson correlation coefficients for each criterion, for both  
 11 the individual stations and the entire dataset. In total 95% of the solutions were retained  
 12 following this approach.

13 The offline-AMS PMF analysis provides the water-soluble contribution of the identified  
 14 aerosol sources. In order to rescale the water-soluble organic carbon concentration of a  
 15 generic factor  $z$  (WSZOC) to its total OC concentration (ZOC) we used the factor recoveries  
 16 ( $R_z$ ) determined by Daellenbach et al. (2016) according to Eq. (5):

$$17 \quad \text{ZOC}_i = \frac{\text{WSZOC}_i}{R_z} \quad (5)$$

18 For each PMF factor (BBOA, W-OOA, and S-OOA), the water-soluble organic carbon  
 19 contribution was determined from the OM:OC ratio calculated from the (water-soluble) factor  
 20 mass spectrum (Aiken et al. 2008). For LOA, whose recovery was not previously reported,  
 21  $R_{LOA}$  was estimated from a single parameter fit according to Eq. (6)

$$22 \quad \text{OC} = \text{TEOC} + \frac{\text{WSBBOA}}{(\text{OM}/\text{OC})_{\text{WSBBOA}} \cdot R_{\text{BBOA}}} + \frac{\text{WSW-OOA}}{(\text{OM}/\text{OC})_{\text{WS-OOA}} \cdot R_{\text{OOA}}} + \frac{\text{WSS-OOA}}{(\text{OM}/\text{OC})_{\text{WSB-OOA}} \cdot R_{\text{OOA}}} + \frac{\text{WSLOA}}{(\text{OM}/\text{OC})_{\text{LOA}} \cdot R_{\text{LOA}}} \quad (6)$$

23 For each of the 95 retained PMF solutions, Eq. (6) was fitted 100 times by randomly selecting  
 24 a set of 100  $R_{\text{BBOA}}$ ,  $R_{\text{OOA}}$  value combinations from those determined by Daellenbach et al.  
 25 (2016). Each fit was initiated by perturbing the input  $\text{OC}_i$  and  $\text{TEOC}_i$  within their  
 26 uncertainties, assuming a normal distribution of the errors. In order to explore the effect of  
 27 possible bulk extraction efficiency (WSOC/OC) systematic measurement biases on our  $R_z$   
 28 estimates, we also perturbed the OC, WSOC,  $R_{\text{BBOA}}$ , and  $R_{\text{OOA}}$  (Daellenbach et al., 2016)  
 29 inputs. Specifically, we assumed an estimated accuracy bias of 5% for each of the perturbed  
 30 parameters, which corresponds to the OC and WSOC measurement accuracy. In total  $9.5 \cdot 10^3$   
 31 fits were performed (Eq. 6) and we retained only solutions with average OC residuals not



1 statistically different from 0 within  $1\sigma$  for each station individually and for summer and  
2 winter individually ( $\sim 8\%$  of the  $9.5 \cdot 10^3$  fits, Fig. S6). The OC residuals of the accepted  
3 solutions did not manifest a clear correlation with the LOA concentration (Fig. S7), indicating  
4 that the estimated  $R_{LOA}$  was properly fitted, without compensating for unexplained variability  
5 of the PMF model or biases from the other  $R_z$ .  $R_z$  distributions shown in Fig. S8 accounted for  
6 all uncertainties and biases mentioned above.  $R_{LOA,med}$  was estimated to be equal to 0.66 (1<sup>st</sup>  
7 quartile 0.61, 3<sup>rd</sup> quartile 0.69, Fig. S8), while the retained  $R_{BBOA}$  and  $R_{OOA}$  values ( $R_{BBOA,med}$   
8 0.57, 1<sup>st</sup> quartile 0.55, 3<sup>rd</sup> quartile 0.60;  $R_{OOA,med}$  0.84, 1<sup>st</sup> quartile 0.81, 3<sup>rd</sup> quartile 0.88) were  
9 systematically lower than those reported by Daellenbach et al. (2016), reflecting the lower  
10 bulk extraction efficiency (bulk EE = WSOC/OC) measured for this dataset (median = 0.59,  
11 1<sup>st</sup> quartile = 0.51, 3<sup>rd</sup> quartile = 0.72 vs. median = 0.74, 1<sup>st</sup> quartile = 0.66, 3<sup>rd</sup> quartile 0.90 in  
12 Daellenbach et al. (2016)). All the retained  $R_k$  combinations are available at DOI:  
13 doi.org/10.5905/ethz-1007-53.

14 Source apportionment uncertainties ( $\sigma_{S.A.}$ ) were estimated for each sample  $i$  and factor  $z$  as the  
15 standard deviation of all the retained PMF solutions ( $\sim 8\%$  of the  $9.5 \cdot 10^3$  fits). In addition to  
16 the rotational ambiguity of the PMF model (explored by the bootstrap technique) and  $R_Z$   
17 uncertainty, each PMF solution included on average 10 repetitions for each filter sample, and  
18 hence  $\sigma_{S.A.}$  accounted also for measurement repeatability. In this work, the statistical  
19 significance of a factor contribution is calculated based on  $\sigma_{S.A.,z,i}$  (Tables S2 and S3).

#### 20 3.1.4. Sensitivity of PMF to the un-apportioned TEOA fraction

21 Despite representing only a small fraction, the un-apportioned water-soluble TEOA  
22 (WSTEOA) contribution could in theory affect the apportionment of the other sources in the  
23 PMF model. To assess this, we performed a PMF sensitivity analysis by subtracting the  
24 estimated WSTEOA concentration from the input PMF data matrix, and by propagating the  
25 estimated WSTEOA uncertainty (section 3.1.2) in the input error matrices. To estimate the  
26 WSTEOA concentration we assumed  $R_{TEOA}$  of  $0.11 \pm 0.01$  (Daellenbach et al., 2016) and we  
27 used the HOA profile reported by Mohr et al. (2012) as surrogate for the TEOA mass spectral  
28 fingerprint. This approach is equivalent to constraining both the WSTEOA time series and  
29 factor profile. Overall the WSTEOA contribution to WSOM was estimated as  $0.2\%_{avg}$ ,  
30 making a successful retrieval of WSTEOA unlikely (Ulbrich et al., 2009). Consistently, PMF  
31 results obtained from this sensitivity analysis indicated that BBOA and B-OOA were robust,  
32 showing only 1% difference from the average offline-AMS source apportionment results,



1 with BBOA increased and B-OOA decreased. S-OOA and LOA instead showed larger  
2 deviations from the average source apportionment results (S-OOA increased by 8% and LOA  
3 decreased by 15%), yet within our source apportionment uncertainties. These results highlight  
4 the marginal influence of the un-apportioned WSTEOA fraction on the other factors.

5

## 6 3.2 Marker-PMF: measured PM<sub>1</sub> source apportionment

7 In the following section we describe the implementation of source apportionment using  
8 chemical markers (marker-PMF), as well as its optimization and uncertainty assessment. We  
9 discuss the number of factors and the selection of specific constraints to improve the source  
10 separation. Subsequently we discuss the source apportionment rotational uncertainty, and the  
11 sensitivity of our PMF results to the number of source specific markers, and to the assumed  
12 constraints.

### 13 3.2.1 Inputs

14 The marker-PMF yields a source apportionment of the entire measured PM<sub>1</sub> fraction (organic  
15 and inorganic). Measured PM<sub>1</sub> is defined here as the sum of EC, ions measured via IC, and  
16 OM estimated from OC measurements multiplied by the (OM:OC)<sub>*i*</sub> ratio determined from the  
17 offline-AMS PMF results by summing the factor profiles OM:OC ratios weighted by the time  
18 dependent factor relative contributions (rescaled by the recoveries). PMF was used to analyze  
19 a data matrix consisting of selected organic molecular markers, ions measured by IC, EC, and  
20 the remaining OM fraction (OM<sub>res</sub>) calculated as the difference between OM and the sum of  
21 the organic markers already included in the input matrix. The marker-PMF analysis is limited  
22 by the lack of elemental measurements (e.g. metals and other trace elements) typically used to  
23 identify mineral dust and certain anthropogenic sources. All markers showing concentrations  
24 above the detection limits for more than 25% of the samples were selected as input variables  
25 (72 in total). The PMF input matrices contain 67 composite samples (31 for Rūgšteliškis, 29  
26 for Preila, and 7 for Vilnius). The errors (*s<sub>i,j</sub>*) were estimated by propagating for each *j*  
27 variable the detection limits (DL) and the relative repeatability (RR) multiplied by the *x<sub>i,j</sub>*  
28 concentration according to Eq. (7) (Rocke and Lorenzato, 1995):

$$29 \quad s_{i,j} = \sqrt{(DL_j)^2 + (x_{i,j} \cdot RR_{i,j})^2} \quad (7)$$



### 1 3.2.2 Number of factors and constraints

2 We selected a 7-factor solution to explain the variability of the measured PM<sub>1</sub> components.  
3 The retrieved factors were biomass burning (BB), traffic exhaust (TE), primary biological  
4 organic aerosol (PBOA), SO<sub>4</sub><sup>2-</sup>-related secondary aerosol (SA), NO<sub>3</sub><sup>-</sup>-related SA, methane  
5 sulfonic acid (MSA)-related SA, and a Na<sup>+</sup>-rich factor explaining the variability of inorganic  
6 components typically related to resuspension of mineral dust, sea salt, and road salt.

7 We first tested an unconstrained source apportionment. This led to a suboptimal separation of  
8 the aerosol sources, with large mixings of PMF factors associated with contributions of  
9 markers originating from different sources. In particular we observed mixing of BB markers  
10 (e.g. levoglucosan) with fossil fuel combustion markers such as hopanes, as well as with  
11 inorganic ions such as NO<sub>3</sub><sup>-</sup> and Ca<sup>2+</sup>. All these markers, although related to different  
12 emission/formation processes, are characterized by similar seasonal trends, i.e. higher  
13 concentrations during winter than in summer. Specifically, the BB tracers increase during  
14 winter because of domestic heating activity, hopanes presumably because of the accumulation  
15 in a shallower boundary layer and lower photochemical degradation, NO<sub>3</sub><sup>-</sup> because of the  
16 partitioning into the particle phase at low temperatures, and Ca<sup>2+</sup> because winter was the  
17 windiest season and therefore was associated with the most intense resuspension.

18 We subsequently exploited the markers' source-specificity to set constraints for the profiles  
19 output by our model: for each individual source, we treated the contribution of the unrelated  
20 source-specific markers as negligible (e.g. we assumed that TE, SA, Na-rich factor and PBOA  
21 do not contribute to levoglucosan). In contrast, the non-source specific variables were freely  
22 apportioned by the PMF algorithm. In a similar way we set constraints for primary markers  
23 (e.g. K<sup>+</sup> and Ca<sup>2+</sup>) and combustion related markers (e.g. PAHs), which are not source-specific  
24 but the contribution of which can be considered as negligible in the SA factors. In this case  
25 the algorithm can freely apportion these markers to all the primary factors and combustion-  
26 related factors, respectively.

27 In details, EC, PAHs, and methyl-PAHs were constrained to zero in non-combustion sources,  
28 i.e. all profiles but TE and BB. While EC could partially derive from dust resuspension,  
29 literature profiles for this source suggest an EC contribution below 1% (Chow et al., 2003).  
30 This is expected to be also the case here given the distance of the three stations from  
31 residential areas and busy roads. Methoxyphenols and sugar anhydrides, considered to be  
32 unique BB markers, were constrained to zero in all sources but BB. Similarly, hopanes were



1 constrained to zero in all factors but TE. We also assumed no contribution from glucose,  
2 arabitol, mannitol, and sorbitol to all secondary factors, and traffic exhaust. The  $\text{SO}_4^{2-}$   
3 contribution from primary traffic emissions was estimated to be negligible, given the use of  
4 desulfurized fuel for vehicles in Lithuania. Likewise, alkane contributions were assumed to be  
5 zero in the SA factors, similar to the contribution of  $\text{Ca}^{2+}$ ,  $\text{Na}^+$ ,  $\text{K}^+$  and  $\text{Mg}^{2+}$  in the SA factors  
6 and TE.

7 The number of factors was increased until no mixing between source-specific markers for  
8 different aerosol sources/processes was observed any more. Secondary sources instead were  
9 explained by three factors because of the distinct seasonal and site-to-site variability of MSA,  
10  $\text{NO}_3^-$  and  $\text{SO}_4^{2-}$ . Oxalate correlated well with  $\text{NH}_4^+$  ( $R=0.62$ ) and the latter well with the sum  
11 of  $\text{SO}_4^{2-}$  and  $\text{NO}_3^-$  equivalents ( $R=0.98$ ). Note that the aforementioned secondary tracers were  
12 not constrained in any factor with the exception of  $\text{SO}_4^{2-}$  contributions which were assumed to  
13 be negligible in the TE factor. Moreover the 7-factor solution showed unbiased residuals  
14 (residual distribution centered at 0 within  $1\sigma$ ) for all the stations together and for each station  
15 individually, while lower order solutions showed biased residuals for at least one station or all  
16 the stations together.

17 PMF results obtained assuming only the aforementioned constraints returned suboptimal  
18 apportionments of  $\text{OM}_{\text{res}}$  and  $\text{Na}^+$  between the BB and the  $\text{Na}^+$ -rich factor, with unusually  
19 high  $\text{OM}_{\text{res}}$  fractional contributions in the  $\text{Na}^+$ -rich factor and unusually high  $\text{Na}^+$   
20 contributions in the BB profile in comparison with literature profiles (Chow et al., 2003;  
21 Huang et al., 2014 and references therein; Schauer et al., 2001). Similarly the EC/ $\text{OM}_{\text{res}}$  value  
22 for TE was substantially lower than literature profiles (El Haddad et al., 2013 and references  
23 therein). Other constraints were therefore introduced to improve the separation of these three  
24 variables. Specifically, EC and  $\text{OM}_{\text{res}}$  were constrained in the traffic profile to be equal to  
25 0.45 and 0.27 ( $a$ -value = 0.5) according to El Haddad et al. (2013), while EC was constrained  
26 to 0.1 ( $a$ -value = 1) in the BB profile according to Huang et al. (2014) and references therein.  
27  $\text{Na}^+$  was constrained to 0.2% ( $a$ -value = 1) in BB according to Schauer et al. (2001), while  
28  $\text{OM}_{\text{res}}$  was constrained to zero in the  $\text{Na}^+$ -rich factor to avoid mixing with BB. Although this  
29 represents a strict constraint, we preferred avoiding constraining  $\text{OM}_{\text{res}}$  to a specific value for  
30 the  $\text{Na}^+$ -rich factor which could not be linked to a unique source but possibly represents  
31 different resuspension-related sources (e.g. sea salt, mineral dust and road dust). However, we  
32 expect none of the aforementioned sources to explain a large fraction of the submicron  $\text{OM}_{\text{res}}$





1 (the OC:dust ratio for dust profiles is 1-15% according to Chow et al., 2003). The sensitivity  
2 of our source apportionment to the constraints listed in this section is discussed in the next  
3 section.

4

### 5 3.2.3. Source apportionment uncertainty and sensitivity analyses

6 We explored the model rotational uncertainty by performing 20 bootstrap PMF runs, and by  
7 perturbing each input  $x_{i,j}$  element within  $2 \cdot s_{i,j}$  assuming a normal distribution of the errors.  
8 Results and uncertainties of the PMF model reported in this paper represent the average and  
9 the standard deviation of the bootstrap runs.

10 We tested the sensitivity of our solution to the constraints listed in section 3.2.2. All the  
11 constraints assuming variable contributions equal to zero were loosened, assuming for each  
12 variable a contribution equivalent to 50%, 37.5%, 25%, and 12.5% of its average relative  
13 contribution to measured  $PM_{10}$ . In all cases the  $a$ -value was set to 1. As expected, results  
14 showed better agreement with the fully constrained solution in the cases of stronger  
15 constraints, meaning that the highest agreements were observed for the 12.5% case both in  
16 terms of mass balance and factor time-series correlations (Fig. S9). The average factor  
17 concentrations for the 12.5% case and the fully constrained average bootstrap PMF solutions  
18 were not statistically different (confidence interval of 95%). Statistically significant  
19 differences arose for the of the  $SO_4^{2-}$ -related SA in the 50% and 37.5% cases, and the  $Na^+$ -  
20 rich factor in the 25% and 37.5% cases, indicating that loosening the constraints allowed  
21 additional rotational uncertainty in comparison to the uncertainty explored by the bootstrap  
22 approach. By contrast, the factors associated with large relative uncertainties from the marker  
23 source apportionment (TE and PBOA, Table S3) showed the best agreement in terms of  
24 concentrations (Fig. S9) with the fully constrained solution, suggesting that the variability  
25 introduced by loosening the constraints did not exceed that already accounted for by the  
26 bootstrap approach. As previously mentioned, the largest contribution discrepancies were  
27 observed for the  $SO_4^{2-}$ -related SA and  $Na^+$ -rich factor. Looser constraints increased the  
28 explained variability of primary components such as EC, arabinol, sorbitol,  $K^+$ ,  $Mg^{2+}$ , and  
29  $Ca^{2+}$  by the (secondary)  $SO_4^{2-}$ -related SA factor. The  $Na^+$ -rich factor showed increasing  
30 contributions from  $OM_{res}$  and from BB components such as methoxyphenols, and anhydrous  
31 sugars, which exhibited similar seasonal trends as the  $Na^+$ -rich factor. None of the marker-  
32 PMF factors showed statistically different average contributions (confidence interval of 95%)



1 when tolerating a variability of the constrained variables within 12.5% of their relative  
2 contribution to  $PM_{10}$ . Note that with this degree of tolerance the contribution of OM to the  
3  $Na^+$ -rich was 28%, which is unrealistically high compared to typically reported values for  
4 OM:dust ratios (<15% Chow et al., 2003). Therefore, we consider the fully constrained PMF  
5 solution to represent best the average composition of the contributing sources.

6 The marker-PMF source apportionment depends strongly on the input variables (i.e. measured  
7 markers), as these are assumed to be highly source specific. That is, minor sources, such as  
8 MSA-related SA and PBOA, are separated because source-specific markers were used as  
9 model inputs. Meanwhile, more variables were used as tracers for TE and BB  
10 (methoxyphenols (5 variables), sugar anhydrides (3 variables), and hopanes (5 variables)),  
11 which gives more weight to these specific sources. We explored the sensitivity of the PMF  
12 results to the number and the choice of traffic and wood burning markers, by replacing them  
13 with randomly selected input variables. In total 20 runs were performed and the average  
14 contribution of the different sources to  $OM_{res}$  was compared with the marker source  
15 apportionment average results, where bootstrap was applied to resample time points. Results  
16 displayed in Fig. S10 are in agreement the apportionment of  $OM_{res}$  from BB within 11%<sub>avg</sub>,  
17 highlighting its robustness. The agreement for TE was lower, which is not surprising given  
18 the lower contribution of this source and the smaller number of specific markers (hopanes).  
19 However, these uncertainties were within the marker source apportionment uncertainty (Fig.  
20 S10), implying that the results were not significantly sensitive to the number and the choice of  
21 input markers for BB and traffic exhaust.

22

## 23 **4 Results and Discussion**

### 24 **4.1 $PM_{10}$ composition**

25 An overview of the measured  $PM_{10}$  composition can be found in Fig. 1. Measured  $PM_{10}$   
26 average concentrations were in general low, with lower values detected at the rural terrestrial  
27 site of Rūgštelīškis ( $5.4 \mu g m^{-3}_{avg}$ ) than in Vilnius ( $6.7 \mu g m^{-3}_{avg}$ ) and Preila ( $7.0 \mu g m^{-3}_{avg}$ ).  
28 OM represented the major fraction of measured  $PM_{10}$  for all seasons and stations, with 57%<sub>avg</sub>  
29 of the mass. The average OM concentrations were higher during winter ( $4.2 \mu g m^{-3}$ ) than in  
30 summer ( $3.0 \mu g m^{-3}$ ) at all sites probably to a combination of domestic wood burning activity  
31 and accumulation of the emissions in a shallower boundary layer. For similar reasons, EC



1 average concentrations showed higher values during winter ( $0.42 \mu\text{g m}^{-3}$ ) than in summer  
2 ( $0.25 \mu\text{g m}^{-3}$ ). During summer, the average EC concentration was  $\sim 5$  times higher in Vilnius  
3 ( $0.54 \mu\text{g m}^{-3}$ ) than in Preila and Rūgštelėškis ( $0.12$  and  $0.11 \mu\text{g m}^{-3}$ , respectively), indicating  
4 an enhanced contribution from combustion emissions. In the absence of domestic heating  
5 during this period, a great part of these emissions may be related to traffic. During winter, EC  
6 concentrations were comparable at all sites (only 25% higher in Vilnius than in Preila and  
7 Rūgštelėškis). This suggests that a great share of wintertime EC may be related to BB, the  
8 average contribution of which is significant at all stations within  $3\sigma$  (table S2). It should be  
9 noted that the highest measured  $\text{PM}_{10}$  concentrations were detected at the remote rural coastal  
10 site of Preila during three different pollution episodes. In particular, the early March episode  
11 corresponded to the period analyzed by Ulevicius et al. (2015) and Dudoitis et al. (2015), and  
12 was attributed to regional transport of polluted air masses associated to an intense land  
13 clearing activity characterized by large scale grass burning in the neighboring Kaliningrad  
14 region.  $\text{SO}_4^{2-}$  represented the second major component of measured  $\text{PM}_{10}$  ( $20\%_{\text{med}}$ ) at all sites  
15 and seasons. Its average concentration remained rather constant with only slightly higher  
16 concentrations in summer than in winter ( $1.2 \pm 0.7 \mu\text{g m}^{-3}$ , and  $1.1 \pm 0.6 \mu\text{g m}^{-3}$  respectively).  
17 Overall  $\text{SO}_4^{2-}$  concentrations did not show large differences from site-to-site, suggestive of  
18 regional sources. By contrast  $\text{NO}_3^-$  showed a clear seasonality with larger contributions in  
19 winter (average  $0.9 \pm 0.8 \mu\text{g m}^{-3}$  equivalent to 12% of measured  $\text{PM}_{10}$ ) than in summer  
20 ( $0.03 \pm 0.03 \mu\text{g m}^{-3}$ ), as expected from its semi-volatile nature.

## 21 4.2 OM source apportionment (Offline-AMS PMF)

22 The apportioned PMF factors were associated to aerosol sources/processes according to their  
23 mass spectral features, seasonal contributions and correlations with tracers. The four  
24 identified factors were BBOA, LOA, B-OOA, and S-OOA, which are thoroughly discussed  
25 below. The TEOA contributions instead were determined using a CMB approach.

26 BBOA was identified by its mass spectral features, with high contributions of  $\text{C}_2\text{H}_4\text{O}_2^+$ , and  
27  $\text{C}_3\text{H}_5\text{O}_2^+$  (Fig. 2), typically associated with levoglucosan fragmentation from cellulose  
28 pyrolysis (Alfarra et al., 2007), accordingly the BBOA factor time series correlated well with  
29 levoglucosan (Pearson correlation coefficient:  $R=0.90$ , Fig. S11). BBOA contributions were  
30 higher during winter and lower during summer (Fig. 3a). We determined the biomass burning  
31 organic carbon (BBOC) concentration from the BBOA time series divided by the



1 OM:OC<sub>BBOA</sub> ratio determined from the corresponding HR spectrum. The winter  
2 levoglucosan/BBOC ratio was 0.16<sub>med</sub>, consistent with values reported in continental Europe  
3 for ambient BBOC profiles (Zotter et al., 2014; Minguillón et al., 2011; Herich et al., 2014).

4 The second factor was defined as LOA because of its statistically significant contribution  
5 (within 3σ) only in Vilnius during summer (table S2), in contrast to other potentially local  
6 primary (e.g. BBOA) and secondary (S-OOA) sources which contributed at all sites. The  
7 LOA mass spectrum was characterized by a high contribution of N-containing fragments  
8 (especially C<sub>5</sub>H<sub>12</sub>N<sup>+</sup>, and C<sub>3</sub>H<sub>8</sub>N<sup>+</sup>), with the highest N:C ratio (0.049) among the apportioned  
9 PMF factors (0.029 for BBOA, 0.013 for S-OOA, 0.023 for B-OOA). A similar factor was  
10 also observed by Byčėnkiėnė et al. (2016) using an ACSM at the same station. In that work,  
11 high LOA concentrations were associated with wind directions from N-NW, and the authors  
12 suggested the sludge utilization system of Vilnius (UAB Vilniausvandenys) situated 3.9 km  
13 NW from the sampling station as a probable source.

14 Two different OOA sources (S-OOA and B-OOA) were resolved and exhibited different  
15 seasonal trends. Separation and classification of OOA sources from offline-AMS is typically  
16 different from that of online AMS and ACSM measurements, mainly due to the different time  
17 resolution. Online-AMS OOA factors are commonly classified based on their volatility (semi-  
18 volatile OOA and low-volatility OOA). This differentiation is typically achieved only for  
19 summer datasets when the temperature gradient between day and night is sufficiently high,  
20 yielding a detectable daily partitioning cycle of the semi-volatile organic compounds and  
21 NO<sub>3</sub><sup>-</sup> between the gas and the particle phases. Online AMS datasets have higher time  
22 resolution than filter sampling, but sampling periods typically cover only a few weeks.  
23 Therefore the apportionment is driven by daily variability rather than seasonal differences. By  
24 contrast, in the offline-AMS source apportionment, given the 24-h time resolution of the filter  
25 sampling and the yearly cycle time coverage, the separation of the factors is driven by the  
26 seasonal variability of the sources and by the site-to-site differences. Therefore, the offline-  
27 AMS source apportionment separates factors by seasonal trends rather than volatility.

28 The resolved B-OOA factor explained a higher fraction than S-OOA. It was associated with  
29 background oxygenated aerosols as no systematic seasonal pattern was observed. However,  
30 B-OOA correlated well with NH<sub>4</sub><sup>+</sup> (*R*=0.69, Fig. S11), and had the highest OM:OC ratio  
31 among the apportioned PMF factors (2.21).



1 Unlike B-OOA, S-OOA showed a clear seasonality with higher contributions during summer,  
2 increasing exponentially with the average daily temperature (Fig. S12a). During summer the  
3 site-to-site S-OOA concentrations were not statistically different within a confidence interval  
4 of 95%, while during winter the site-to-site agreement was lower, possibly due to the larger  
5 model uncertainty associated with the low S-OOA concentrations. A similar S-OOA vs.  
6 temperature relationship was reported by Leaitch et al. (2011) for a terpene dominated  
7 Canadian forest using an ACSM and by Daellenbach et al. (2016) and Bozzetti et al. (2016)  
8 for the case of Switzerland (Fig. S12b), using a similar source apportionment model. This  
9 increase in S-OOA concentration with temperature is consistent with the exponential increase  
10 in biogenic SOA precursors (Guenther et al., 2006). Therefore, even though the behavior of S-  
11 OOA at different sites might be driven by several parameters, including vegetation coverage,  
12 available OA mass, air masses photochemical age and ambient oxidation conditions (e.g. NO<sub>x</sub>  
13 concentration), temperature seems to be the main driver of S-OOA concentrations. Overall  
14 more field observations at other European locations are needed to validate this relation. While  
15 the results indicate a probable secondary biogenic origin of the S-OOA factor, the precursors  
16 of the B-OOA factor are not identified. In section 4.4.2 more insights into the OOA sources  
17 will be discussed.

18 The S-OOA profile showed a CO<sub>2</sub><sup>+</sup>/C<sub>2</sub>H<sub>3</sub>O<sup>+</sup> ratio of 0.61<sub>avg</sub>, placing it in the region of semi-  
19 volatile SOA from biogenic emissions in the *f*<sub>44</sub>/*f*<sub>43</sub> space (Ng et al., 2011), as attributed by  
20 Canonaco et al. (2015). Despite the higher summer photochemical activity, the water-soluble  
21 bulk OA showed more oxidized mass spectral fingerprints during winter (O:C=0.61<sub>avg</sub>) than  
22 in summer (O:C=0.55<sub>avg</sub>), similar to the results presented by Canonaco et al. (2015) for  
23 Zurich. Accordingly, the S-OOA profile also showed a less oxidized water-soluble mass  
24 spectral fingerprint than B-OOA, with an O:C ratio of 0.40<sub>avg</sub>, in comparison with 0.80<sub>avg</sub> for  
25 B-OOA. Considering the sum of B-OOA and S-OOA, the median OOA:NH<sub>4</sub><sup>+</sup> ratios for  
26 Rūgštelīškis, Preila, and Vilnius were 3.2, 2.4, and 2.5 respectively, higher than the average  
27 but within the range of the values reported by Crippa et al. (2014) for 25 different European  
28 rural sites (2.0<sub>avg</sub>; minimum value 0.3; maximum 7.3).

29

### 30 4.3 PM<sub>1</sub> source apportionment (marker-PMF)

31 The PMF factors in this analysis were associated with specific aerosol sources/processes  
32 according to their profiles, seasonal trends and relative contributions to the key variables. Fig.



1 4 displays factor profiles, and the relative contribution of each factor to each variable. The  
2 Na<sup>+</sup>-rich factor explained a large part of the variability of Ca<sup>2+</sup>, Mg<sup>2+</sup>, and Na<sup>+</sup> (Fig. 4) and  
3 showed higher contributions during winter than in summer, suggesting a possible  
4 resuspension of sand and salt typically used during winter in Lithuania for road de-icing. This  
5 seasonal trend is also consistent with wind speed, which showed the highest monthly values  
6 during December 2013 and January 2014. We cannot exclude the possibility that this factor  
7 may include contributions from sea salt, although Na<sup>+</sup> and Cl<sup>-</sup> were not enhanced at the  
8 marine station in comparison with the other stations. The overall contribution of this Na<sup>+</sup>-rich  
9 factor to measured PM<sub>1</sub> was relatively small (1%<sub>avg</sub>), but may be larger in the coarse fraction.

10 The BB factor showed a well-defined seasonality, with high contributions during winter. This  
11 factor explained a large part of the variability of typical wood combustion tracers such as  
12 methoxyphenols, sugar anhydrides (including levoglucosan, mannosan, and galactosan), K<sup>+</sup>,  
13 Cl<sup>-</sup>, EC, PAHs, and methyl-PAHs (Fig. 4). Using the ratio (1.88) calculated from offline-  
14 AMS, we estimated the levoglucosan:BBOC ratio to be 0.18<sub>avg</sub>, which is within the range of  
15 previous studies (Ulevicius et al., 2015 and references therein). Note that this factor explained  
16 also large fractions of variables typically associated with non-vehicular fossil fuel  
17 combustion, such as benzo(b)naphtho(2,1-d)thiophene (BNT[2,1]) and 6,10,14-trimethyl-2-  
18 pentadecanone (DMPT, Fig. 4, Manish et al., 2007; Subramanian et al., 2007), indicating a  
19 potential mixing of BB with fossil fuel combustion sources. However, the fossil fuel  
20 combustion contribution to BB is unlikely to be large, considering the low concentrations of  
21 fossil fuel tracers such as hopanes (66% of the samples below quantification limit (<QL)),  
22 BNT[2,1] (64%<QL), and DMPT (55%<QL). Moreover, the above mentioned agreement of  
23 the levoglucosan:BBOC ratio with previous studies corroborates the BB estimate from the  
24 marker-PMF.

25 The traffic exhaust factor explained a significant fraction of the alkane variability, with a  
26 preferential contribution from light alkanes (Fig. 4). Its contribution was statistically  
27 significant within 1σ only for one filter collected in Vilnius. However on average the  
28 concentration was higher in Vilnius than at the other stations and in general higher in winter  
29 than in summer.

30 The PBOA factor explained the variability of the primary biological components, such as  
31 glucose, mannitol, sorbitol, arabitol, and alkanes with an odd number of carbon atoms  
32 (consistent with Bozzetti et al., 2016 and references therein). Highest PBOA concentrations



1 were observed during spring, especially at the rural site of Rūgšteliškis. Overall the  
2 contribution of this factor was uncertain with an average relative model error of 160%  
3 probably due to the small PBOA contributions ( $0.6\%_{\text{avg}}$  of the total OM), which hampers a  
4 more precise determination by the model. In particular  $\text{OM}_{\text{res}}$  was the variable showing the  
5 highest mass contribution to the PBOA factor. However, the large contribution and the large  
6 uncertainty of  $\text{OM}_{\text{res}}$  to this factor ( $0.3\pm 0.4$ ) resulted in a large uncertainty in the PBOA  
7 estimated concentration.

8 The last three factors were related to SA, as indicated by the large contributions of secondary  
9 species such as oxalate,  $\text{SO}_4^{2-}$ , MSA, and  $\text{NO}_3^-$  to the factor profiles (Fig. 4). The three factors  
10 showed different spatial and temporal contributions.

11 The  $\text{NO}_3^-$ -related SA exhibited highest contributions during winter, suggesting temperature-  
12 driven partitioning of secondary aerosol components. Moreover the  $\text{NO}_3^-$ -related SA,  
13 similarly to BB and TE, showed the highest concentrations in Vilnius, and the lowest in  
14 Rūgšteliškis suggesting its possible relation with anthropogenic gaseous precursors (e.g.  
15  $\text{NO}_x$ ).

16 The MSA-related SA factor manifested the highest concentrations at the marine site of Preila  
17 during summer, and in general larger contributions during summer than winter, suggesting its  
18 relation with marine secondary aerosol. MSA has been reported to be related to marine  
19 secondary biogenic emissions deriving from the photo-oxidation of dimethyl sulfide (DMS)  
20 emitted by the phytoplankton bloom occurring during the warm season (Li et al., 1993,  
21 Crippa et al., 2013 and references therein).

22 The last factor ( $\text{SO}_4^{2-}$ -related SA) showed higher contributions during summer than in winter  
23 without clear site-to-site variability, following the seasonal behavior of  $\text{SO}_4^{2-}$  showing slightly  
24 higher concentrations during summer than in winter, which is probably driven by the  
25 secondary formation from gaseous photochemical reactions and aqueous phase oxidation.  
26 This factor explained the largest part of the oxalate and  $\text{SO}_4^{2-}$  variability and represented  
27  $48\%_{\text{avg}}$  of the measured  $\text{PM}_{10}$  by mass.

#### 28 **4.4 Comparison of the source apportionment methods**

29 In this section we compare the offline-AMS PMF and marker-PMF results. We begin with  
30 BBOA and TE emissions which were resolved by both approaches. The remaining OM  
31 fraction (Other-OA) was apportioned by the offline-AMS source apportionment to B-OOA,





1 S-OOA and LOA (Other-OA<sub>offline-AMS</sub>). However, the LOA contribution was statistically  
2 significant (within  $3\sigma$ ) only in Vilnius during summer (Table S2), while no data were  
3 available for these periods from the marker source apportionment. The marker source  
4 apportionment instead attributed the Other-OA mass fraction to 4 factors (Other-OA<sub>marker</sub>):  
5 PBOA, as well as to  $\text{SO}_4^{2-}$ ,  $\text{NO}_3^-$ , and MSA-related secondary organic aerosols (SOA, Fig.  
6 S13). The OA concentrations of the factors retrieved from the PM<sub>1</sub> markers source  
7 apportionment were obtained by multiplying the factor time series by the sum of the organic  
8 markers and OM<sub>res</sub> contributions to the normalized factor profiles. The PM concentrations  
9 from the marker PMF factors are displayed in Fig. 5.

#### 10 4.4.1 Primary OA sources

11 Offline-AMS and marker source apportionments provided comparable BBOA estimates, with  
12 concentrations agreeing within a 95% confidence interval (Fig. 6). Results revealed that  
13 BBOA contributed the largest fraction to the total OM during winter in Preila and Vilnius,  
14 while in Rūgšteliškis the largest OA source derived from B-OOA. The average winter BBOA  
15 concentration was  $1.1 \pm 0.8 \mu\text{g m}^{-3}$  in Rūgšteliškis and  $2 \pm 1 \mu\text{g m}^{-3}$  in Vilnius (errors in this  
16 section represent the standard deviation of the temporal variability). Overall the average  
17 BBOA concentrations were higher at the urban background site of Vilnius and lower at the  
18 rural terrestrial site of Rūgšteliškis. Preila showed the highest values ( $3 \pm 3 \mu\text{g m}^{-3}$ ) driven by  
19 the grass burning episode occurred at the beginning of March (Ulevicius et al., 2016).  
20 Excluding this episode, the BBOA winter concentration was lower than in Vilnius ( $1.8 \mu\text{g m}^{-3}$ ).  
21 During winter, Preila and Vilnius showed well correlated BBOA time series ( $R=0.91$ ).  
22 These results highlight the important role of regional meteorological conditions on the air  
23 quality in the south east Baltic region.

24 By contrast, during summer BBOA concentrations were much lower, with 40% of the points  
25 showing statistically not significant contributions within  $3\sigma$  for the offline-AMS source  
26 apportionment and 100% for the marker source apportionment. Between late autumn and  
27 early March the offline-AMS source apportionment revealed three simultaneous episodes  
28 with high BBOA concentrations at the three stations, while the marker source apportionment  
29 which is characterized by lower time resolution did not capture some of these episodes. The  
30 first episode occurred between 19 and 25 December 2013 during a cold period with an  
31 average daily temperature drop to  $-9.7 \text{ }^\circ\text{C}$  as measured at the Rūgšteliškis station (no





1 temperature data were available for the other stations). The third episode occurred between 5  
2 and 10 March 2014 and was associated with an intense grass burning episode localized mostly  
3 in the Kaliningrad region (Ulevicius et al., 2015, Dudoitis et al., 2015, Mordas et al., 2016).  
4 The episode was not associated with a clear temperature drop, with the highest concentration  
5 ( $14 \mu\text{g m}^{-3}$ ) found at Preila on 10 March 2014, the closest station to the Kaliningrad region.  
6 Similarly, at the beginning of February high BBOA concentrations were registered at the  
7 three stations, without a clear temperature decrease. Other intense BBOA events were  
8 detected but only on a local scale, with intensities comparable to the regional scale episodes.  
9 Using the OM:OC<sub>BBOA</sub> ratio calculated from the HR water-soluble BBOA spectrum (1.88),  
10 we estimated the BBOC<sub>avg</sub> concentrations during the grass burning episode (5-10 March  
11 2014) to span between 0.8 and  $7.2 \mu\text{g m}^{-3}$ . On a daily basis our BBOC concentrations are  
12 consistent with the estimated ranges reported by Ulevicius et al. (2015) for non-fossil primary  
13 organic carbon, showing also a high correlation ( $R=0.98$ ).

14 TEOA estimates obtained by offline-AMS and marker-PMF agreed well with each other, with  
15 99% of the points being not statistically different within  $1\sigma$  (Fig. 6). The two approaches  
16 confirm that TEOA is a minor source at all three stations with on average higher  
17 concentrations in Vilnius (up to  $0.8 \mu\text{g m}^{-3}$ ), than in Preila and Rūgšteliškis (up to  $0.2 \mu\text{g m}^{-3}$ ).  
18 Hopane concentrations were below detection limits ( $7 \text{ pg m}^{-3}$ ) for 66% of the collected  
19 samples. TEOA, similarly to hopanes and  $\text{NO}_x$ , showed a clear spatial and seasonal variability  
20 with higher concentrations in Vilnius during winter, suggesting an accumulation of traffic  
21 emissions in a shallower boundary layer (Fig. 3b,  $\text{NO}_x$  data available only for Vilnius).  
22 During the grass burning event, we observed a peak in the total hopane concentration, and  
23 therefore also a peak of the estimated TEOA ( $2.4 \mu\text{g m}^{-3}$  maximum value). This relatively  
24 high concentration is most probably not due to a local increase of TE, but rather due to a  
25 regional transport of polluted air masses from neighboring countries (Poland and the Russian  
26 Kaliningrad enclave). By assuming an OM:OC<sub>TEOA</sub> ratio of  $1.2\pm 0.1$  (Aiken et al., 2008, Mohr  
27 et al., 2008, Docherty et al., 2011, Setyan et al., 2012), we determined the corresponding  
28 organic carbon content (TEOC). Our TEOC concentration was consistent within  $1\sigma$  with the  
29 average fossil primary OC over the whole episode estimated by Ulevicius et al. (2015),  
30 although on a daily basis the agreement was relatively poor.

31 Overall, the offline-AMS source apportionment and the marker-PMF returned comparable  
32 results for TEOA and BBOA emissions, therefore not surprisingly the two approaches yielded



1 OA concentrations also for the Other-OA fractions which agreed within  $1\sigma$  for 90% of the  
2 points (Figure 6). This agreement was better for Rūgšteliškis and Preila (94% and 90%,  
3 respectively of the points not statistically different within  $1\sigma$ ), and worse for Vilnius (71% of  
4 the points not statistically different within  $1\sigma$ ).

#### 5 4.4.2 Other-OA sources: offline-AMS and marker-source apportionment 6 comparison

7 The marker-source apportionment, in comparison to the offline-AMS source apportionment  
8 enables resolving well-correlated sources (e.g. BBOA and  $\text{NO}_3^-$ -related SOA) as well as  
9 minor sources (e.g. MSA-related SOA and PBOA) because source-specific markers were  
10 used as model inputs. By contrast, the offline-AMS source apportionment is capable of  
11 resolving OA sources for which no specific markers were available such as LOA, which was  
12 separated due to the distinct spatial and temporal trends of some N-containing AMS  
13 fragments. We first briefly summarize the Other-OA factor concentrations and their site-to-  
14 site differences retrieved by the two techniques; subsequently we compare the two source  
15 apportionment results.

16 The Other-OA<sub>offline-AMS</sub> factor time series are displayed in Fig. S13. The B-OOA factor  
17 showed relatively stable concentrations throughout the year with  $0.9 \pm 0.8_{\text{avg}} \mu\text{g m}^{-3}$  during  
18 summer and  $1.1 \pm 0.9_{\text{avg}} \mu\text{g m}^{-3}$  during winter. Although B-OOA concentrations were relatively  
19 stable throughout the year, higher contributions were observed in Preila and Rūgšteliškis  
20 compared to Vilnius. The extreme average seasonal concentrations were between 0.8 and 1.3  
21  $\mu\text{g m}^{-3}$  at Rūgšteliškis during fall and winter, between 0.9 and 1.1  $\mu\text{g m}^{-3}$  at Preila during  
22 spring and winter, and between 0.4 and 0.6  $\mu\text{g m}^{-3}$  in Vilnius during summer and winter.  
23 These values do not evidence clear seasonal trends, but highlight a site-to-site variability  
24 which will be further discussed in the following. S-OOA instead was the largest contributor to  
25 total OM during summer with an average concentration of  $1.2 \pm 0.8 \mu\text{g m}^{-3}$ , always agreeing  
26 between sites within a confidence interval of 95% (2 tails t-test). By contrast, during winter  
27 the S-OOA concentration dropped to an average value of  $0.3 \pm 0.2 \mu\text{g m}^{-3}$ , with 81% of the  
28 points not statistically different from  $0 \mu\text{g m}^{-3}$  within  $3\sigma$ . Finally, the LOA factor showed  
29 statistically significant contributions within  $3\sigma$  only during summer and late spring in Vilnius.  
30 Despite its considerable day-to-day variability this fraction contributed  $1.0 \pm 0.8 \mu\text{g m}^{-3}_{\text{avg}}$  in  
31 Vilnius during summer.



1 The markers source apportionment instead attributed 85%<sub>avg</sub> of the Other-OA<sub>marker</sub> mass to the  
 2 SO<sub>4</sub><sup>2-</sup>-related SOA, while NO<sub>3</sub><sup>-</sup>-related SOA, MSA-related SOA, and PBOA explained  
 3 respectively 9%<sub>avg</sub>, 5%<sub>avg</sub> and 1%<sub>avg</sub> of the Other-OA<sub>marker</sub> mass (Fig. S13). The SO<sub>4</sub><sup>2-</sup>-related  
 4 SOA average concentration was 2.4 μg m<sup>-3</sup> during summer and 1.7 μg m<sup>-3</sup> during winter with  
 5 no significant differences from station to station, suggesting a regional origin of the factor.  
 6 The NO<sub>3</sub><sup>-</sup>-related SOA concentration was 0.4 μg m<sup>-3</sup><sub>avg</sub> during winter, only 0.03<sub>avg</sub> μg m<sup>-3</sup>,  
 7 during summer, corresponding to 10%<sub>avg</sub> and 1% of the OA, respectively. Moreover, the NO<sub>3</sub><sup>-</sup>  
 8 -related SOA during winter showed the highest average concentrations in Vilnius with 0.5 μg  
 9 m<sup>-3</sup> and the lowest in Rūgštelėškis with 0.3 μg m<sup>-3</sup><sub>avg</sub>. The MSA-related SOA instead  
 10 manifested the highest concentrations during summer with an average of 0.12 μg m<sup>-3</sup><sub>avg</sub>.  
 11 Higher values were observed during summer at the rural coastal site of Preila where the  
 12 average concentration was 0.28 μg m<sup>-3</sup><sub>avg</sub> corresponding to 10%<sub>avg</sub> of the OM. Finally, the  
 13 PBOA factor exhibited the largest seasonal concentrations during spring at the rural terrestrial  
 14 site of Rūgštelėškis with an average of 0.05 μg m<sup>-3</sup><sub>avg</sub>, while the summer average  
 15 concentration was 0.02 μg m<sup>-3</sup> consistent with the low PBOA estimates reported in Bozzetti et  
 16 al. (2016) for the submicron fraction during summer.

17 Many previous studies reported a source apportionment of organic and inorganic markers  
 18 concentrations (Viana et al., 2008 and references therein). In these studies SO<sub>4</sub><sup>2-</sup>, NO<sub>3</sub><sup>-</sup>, and  
 19 NH<sub>4</sub><sup>+</sup> were typically used as tracers for secondary aerosol factors commonly associated with  
 20 regional background and long-range transport; here we compare the apportionment of the  
 21 SOA factors obtained from the marker source apportionment and the OOA factors separated  
 22 by the offline-AMS source apportionment. Moreover, contrasting the two source  
 23 apportionments may provide insight into the origin of the OOA factors retrieved from the  
 24 offline-AMS source apportionment, and into the origin of the SOA factors resolved by the  
 25 offline-AMS source apportionment. To our knowledge an explicit comparison has not yet  
 26 been reported in the literature.

27

28 Table 2: Pearson correlation coefficients between Other-OA components from offline-AMS  
 29 and marker-source apportionment.

		Other-OA <sub>marker</sub>			
		SO <sub>4</sub> <sup>2-</sup> -related SOA	MSA-related SOA	NO <sub>3</sub> <sup>-</sup> -related SOA	PBOA
Other- OA <sub>offline</sub>	LOA	0.33	0.16	-0.08	0.10
	B-OOA	0.70	0.22	0.21	0.47



AMS	S-OOA	0.60	0.45	-0.47	0.05
-----	-------	------	------	-------	------

1

2 Table 2 reports the correlations between the time series of the Other-OA<sub>marker</sub> factors and the  
 3 Other-OA<sub>offline-AMS</sub> factors (Figs. 6 and S13). These correlations are mostly driven by seasonal  
 4 trends as none of these sources shows clear spikes except for LOA during summer in Vilnius.  
 5 Using the correlations coefficients we can identify the mostly related factors from the two  
 6 source apportionments.

7 The SO<sub>4</sub><sup>2-</sup>-related SOA explained the largest fraction of the Other-OA<sub>marker</sub> mass (85%<sub>avg</sub>),  
 8 and it was the only Other-OA<sub>marker</sub> factor always exceeding the individual concentrations of  
 9 B-OOA and S-OOA, indicating that the variability explained by the SO<sub>4</sub><sup>2-</sup>-related SOA in the  
 10 marker-source apportionment is explained by both OOA factors in the offline-AMS source  
 11 apportionment. Moreover, the SO<sub>4</sub><sup>2-</sup>-related SOA seasonality seems consistent with the sum  
 12 of S-OOA and B-OOA with higher concentrations in summer than in winter. This observation  
 13 suggests that the OOA factors resolved by offline-AMS are mostly of secondary origin and  
 14 the SO<sub>4</sub><sup>2-</sup>-related SOA, typically resolved by the markersource apportionment, explains the  
 15 largest fraction of the OOA factors apportioned by offline-AMS which includes both biogenic  
 16 SOA and aged background OA.

17 The NO<sub>3</sub><sup>-</sup>-related SOA and the PBOA were mostly related to the B-OOA factor as they  
 18 showed higher correlations with B-OOA than with S-OOA. The B-OOA factor therefore may  
 19 explain a small fraction of primary sources (PBOA), which however represents only 0.6%<sub>avg</sub>  
 20 of the total OA.

21 The MSA-related SOA showed the highest correlation with the S-OOA factor, as the two  
 22 sources exhibited the highest concentrations during summer, although the MSA-related SOA  
 23 preferentially contributed at the rural coastal site of Preila. While we already discussed the  
 24 probable secondary biogenic origin of S-OOA, the correlation with the MSA-related SOA  
 25 suggests that the S-OOA factor, especially at the rural coastal site of Preila, explains also a  
 26 large fraction of the marine biogenic SOA. Assuming all the MSA-related SOA to be  
 27 explained by the S-OOA factor, we estimate a marine biogenic SOA contribution to S-OOA  
 28 of 27%<sub>avg</sub> during summer at Preila, while this contribution is lower at the other stations  
 29 (12%<sub>avg</sub> in Rūgštelėškis during summer, 7% in Vilnius during spring, no summer data for  
 30 Vilnius Fig. S13). As already mentioned, here we assume all the MSA-related SOA to be  
 31 related to marine secondary biogenic emissions, however other studies also report MSA from



1 terrestrial biogenic emissions (Jardine et al., 2015), moreover a certain fraction of the MSA-  
2 related SOA can also be explained by the B-OOA factor. Overall these findings indicate that  
3 the terrestrial sources dominate the S-OOA composition, nevertheless the marine SOA  
4 sources may represent a non-negligible fraction, especially at the marine site.

5 Another advantage obtained in coupling the two source apportionment results is the  
6 possibility to study the robustness of the factor analyses by evaluating the consistency of the  
7 two approaches as we already discussed for the primary OA and Other-OA fractions. By  
8 subtracting LOA and S-OOA from Other-OA<sub>marker</sub> we can estimate the equivalent B-OOA  
9 concentration from the marker source apportionment (B-OOA<sub>marker</sub>). Unlike the B-OOA  
10 factor from offline-AMS, whose contribution is lower at Vilnius, B-OOA<sub>marker</sub> did not show  
11 statistically different concentrations at all stations within a confidence interval of 95%. This  
12 discrepancy could indicate some PMF residual uncertainties or biases not considered in our  
13 error estimate for offline-AMS and/or markers source apportionments for Vilnius, which  
14 could not be detected without coupling the 2 source apportionment approaches.

15

#### 16 **4.5 $f\text{CO}^+$ vs. $f\text{CO}_2^+$**

17 Figure 7 displays the water-soluble  $f\text{CO}^+$  vs.  $f\text{CO}_2^+$  scatter plot. A certain correlation ( $R=0.63$ )  
18 is seen, with  $f\text{CO}^+$  values being systematically lower than  $f\text{CO}_2^+$  ( $\text{CO}_2^+:\text{CO}^+$ : 1<sup>st</sup> quartile 1.50,  
19 median 1.75, 3<sup>rd</sup> quartile 2.01), whereas a 1:1  $\text{CO}_2^+:\text{CO}^+$  ratio is assumed in standard  
20 AMS/ACSM analyses (Aiken et al., 2008; Canagaratna et al., 2007). Comparing the measured  
21  $\text{CO}_2^+:\text{CO}^+$  values for the bulk WSOM and for pure gaseous  $\text{CO}_2$  might provide insight into  
22 the origin of the  $\text{CO}^+$  fragment in the AMS. The fragmentation of pure gaseous  $\text{CO}_2$  returned  
23 a  $\text{CO}_2^+:\text{CO}^+$  ratio of 8.21<sub>avg</sub> which is significantly higher than our findings for the water-  
24 soluble bulk OA (1.75<sub>med</sub>) suggesting that the WSOM decarboxylation on the AMS vaporizer  
25 represents only a minor source of  $\text{CO}^+$ .

26 Figure 7b and Fig. 8 show that not only does the water-soluble (WS)  $\text{CO}_2^+:\text{CO}^+$  ratio  
27 systematically differ from 1, but it also varies throughout the year with higher  $\text{CO}_2^+:\text{CO}^+$   
28 values associated with warmer temperatures (Fig. 7b). The lower  $\text{CO}_2^+:\text{CO}^+$  ratios in winter  
29 are primarily due to BB, as the WSBBOA factor profile showed the lowest  $\text{CO}_2^+:\text{CO}^+$  ratio  
30 (1.20<sub>avg</sub>) among all the apportioned WS factors (2.00<sub>avg</sub> for B-OOA, 2.70<sub>avg</sub> for S-OOA, and  
31 2.70<sub>avg</sub> for LOA). We observed a seasonal variation of the  $\text{CO}_2^+:\text{CO}^+$  ratio also for the water-



1 soluble OOA (S-OOA + B-OOA) mass spectral fingerprint. The  $\text{CO}_2^+:\text{CO}^+$  ratio was slightly  
 2 lower for B-OOA than for S-OOA ( $2.00_{\text{avg}}$  for B-OOA, 2.70 for S-OOA). Nevertheless, given  
 3 the low S-OOA relative contribution during winter (Fig. 3), we note that the total OOA  
 4 showed a slightly lower  $\text{CO}_2^+:\text{CO}^+$  ratio during winter than in summer (Fig. S14), indicating  
 5 that the OOA mass spectral fingerprint evolves over the year, possibly because of different  
 6 precursor concentrations, and different photochemical activity.

7 Fig. 7a shows that most of the measured  $\{f\text{CO}^+;f\text{CO}_2^+\}$  combinations lies within the triangle  
 8 defined by the BBOA, S-OOA and B-OOA  $\{f\text{CO}^+;f\text{CO}_2^+\}$  combinations. The LOA factor  
 9  $\{f\text{CO}^+;f\text{CO}_2^+\}$  combination lies within the triangle as well, but is anyways a minor source and  
 10 thus unlikely to contribute to the  $\text{CO}_2^+/\text{CO}^+$  variability. We parameterized the  $\text{CO}^+$  variability  
 11 as a function of the  $\text{CO}_2^+$ , and  $\text{C}_2\text{H}_4\text{O}_2^+$  fragment variabilities using a multi-parameter fit  
 12 according to Eq. (8).  $\text{CO}_2^+$  and  $\text{C}_2\text{H}_4\text{O}_2^+$  were chosen as B-OOA and BBOA tracers,  
 13 respectively, with B-OOA and BBOA being the factors that explained the largest fraction of  
 14 the  $f\text{CO}^+$  variability (85% together).

$$15 \quad \text{CO}^+_i = a \cdot \text{CO}_2^+_{i+} + b \cdot \text{C}_2\text{H}_4\text{O}_2^+_i \quad (8)$$

16 Although this parameterization is derived from the WSOM fraction  $\text{CO}_2^+$ ,  $\text{C}_2\text{H}_4\text{O}_2^+$ , and  $\text{CO}^+$   
 17 originate from the fragmentation of oxygenated, i.e. mostly water-soluble compounds.  
 18 Accordingly, this parameterization might also well represent the total bulk OA (as the offline-  
 19 AMS recoveries of these oxygenated fragments are relatively similar:  $R_{\text{CO}_2^+}=0.74$ ,  
 20  $R_{\text{C}_2\text{H}_4\text{O}_2^+}=0.61$ , Daellenbach et al., 2016). Note that this parameterization may represent very  
 21 well the variation of  $\text{CO}^+$  in an environment impacted by BBOA and OOA, but should be  
 22 used with caution when other sources (such as COA) may contribute to  $\text{CO}^+$ ,  $\text{CO}_2^+$  and  
 23  $\text{C}_2\text{H}_4\text{O}_2^+$ . In order to check the applicability of this parameterization to a PMF output, we  
 24 recommend monitoring the  $\text{CO}_2^+$  and  $\text{C}_2\text{H}_4\text{O}_2^+$  variability explained by the OOA and BBOA  
 25 factors. In case a large part of the  $\text{CO}_2^+$  and  $\text{C}_2\text{H}_4\text{O}_2^+$  variability is explained by OOA and  
 26 BBOA, the parameterization should unlikely return uncertain  $\text{CO}^+$  values. The coefficients  $a$   
 27 and  $b$  of Eq. (8) were determined as 0.52 and 1.39 respectively, while the average fit residuals  
 28 were estimated to be equal to 10% (Fig. S15). In contrast, parameterizing  $\text{CO}^+$  as proportional  
 29 to  $\text{CO}_2^+$  only (as done in the standard AMS analysis scheme with coefficients updated to the  
 30 linear fit between  $\text{CO}^+$  and  $\text{CO}_2^+$  (1.75)) yielded  $20\%_{\text{avg}}$  residuals, indicating that such a  
 31 univariate function describes the  $\text{CO}^+$  variation less precisely.



1 An alternative parameterization is presented in the SI in which the contribution of moderately  
2 oxygenated species (such as S-OOA) to  $\text{CO}^+$  was also considered by using  $\text{C}_2\text{H}_3\text{O}^+$  as an  
3 independent variable. We show that the dependence of  $\text{CO}^+$  on  $\text{C}_2\text{H}_3\text{O}^+$  is statistically  
4 significant (Fig. 7b) as also suggested by the PMF results (S-OOA contributes 12% to the  
5  $\text{CO}^+$  variability). However, the parameter relating  $\text{CO}^+$  to  $\text{C}_2\text{H}_3\text{O}^+$  is negative, because the  
6  $\text{CO}^+:\text{CO}_2^+$  and  $\text{CO}^+:\text{C}_2\text{H}_4\text{O}_2^+$  ratios are lower in moderately oxygenated species compared to  
7 species present in BBOA and B-OOA. While this parameterization captures the variability of  
8  $\text{CO}^+$  across the seasons better compared to a 2-parameter fit for the present dataset, it may be  
9 more prone to biases in other environments due to the known contributions of other factors to  
10  $\text{C}_2\text{H}_3\text{O}^+$ . For example, cooking-influenced organic aerosol (COA) often accounts for a  
11 significant fraction of  $\text{C}_2\text{H}_3\text{O}^+$ . For ambient datasets we propose the use of  $\text{CO}_2^+$  and  $\text{C}_2\text{H}_4\text{O}_2^+$   
12 only, which may capture less variation but is also less prone to biases. Although our results  
13 suggest that the available  $\text{CO}^+$  and O:C estimates (Aiken et al., 2008; Canagaratna et al.,  
14 2015) may not well capture the  $\text{CO}^+$  variability, our  $\text{CO}^+$  parameterization should not be  
15 applied to calculate the O:C ratios or recalculate the OA mass from AMS datasets, as those  
16 are calibrated assuming a standard fragmentation table (i.e.  $\text{CO}_2^+ = \text{CO}^+$ ).

17 In a recent work, Canagaratna et al. (2015) reported the Ar nebulization of water soluble  
18 single compounds to study the HR-AMS mass spectral fingerprints in order to improve the  
19 calculation of O:C and OM:OC ratios. Following the same procedure, we nebulized a subset  
20 of the same standard compounds including malic acid, azalaic acid, citric acid, tartaric acid,  
21 cis-pinonic acid, and D(+)-mannose. We obtained comparable  $\text{CO}_2^+:\text{CO}^+$  ratios (within 10%)  
22 to those of Canagaratna et al. (2015) for all the analyzed compounds, highlighting the  
23 comparability of results across different instruments. With the exception of some  
24 multifunctional compounds, the water-soluble single compounds analyzed by Canagaratna et  
25 al. (2015) mostly showed  $\text{CO}_2^+:\text{CO}^+$  ratios  $<1$ , systematically lower than the  $\text{CO}_2^+:\text{CO}^+$  ratios  
26 measured for the bulk WSOM in Lithuania (1<sup>st</sup> quartile 1.50, median 1.75, 3<sup>rd</sup> quartile 2.01),  
27 which represents a large fraction of the total OM (bulk EE: median = 0.59, 1<sup>st</sup> quartile = 0.51,  
28 3<sup>rd</sup> quartile = 0.72). This indicates that the selection of appropriate reference compounds for  
29 ambient OA is non-trivial, and the investigation of multifunctional compounds is of high  
30 importance.

31





## 1 5 Conclusions

2 PM<sub>1</sub> filter samples were collected over an entire year (November 2013 to October 2014) at  
3 three different stations in Lithuania. Filters were analyzed by water extraction followed by  
4 nebulization of the liquid extracts and subsequent measurement of the generated aerosol with  
5 an HR-ToF-AMS (Daellenbach et al., 2016). For the first time, the nebulization step was  
6 conducted in Ar, enabling direct measurement of the CO<sup>+</sup> ion, which is typically masked by  
7 N<sub>2</sub><sup>+</sup> in ambient air and assumed to be equal to CO<sub>2</sub><sup>+</sup> (Aiken et al., 2008). CO<sub>2</sub><sup>+</sup>:CO<sup>+</sup> values >1  
8 were systematically observed, with a mean ratio of 1.7±0.3. This is likely an upper limit for  
9 ambient aerosol, as only the water-soluble OM fraction is measured by the offline-AMS  
10 technique. CO<sup>+</sup> concentrations were parameterized as a function of CO<sub>2</sub><sup>+</sup>, and C<sub>2</sub>H<sub>4</sub>O<sub>2</sub><sup>+</sup>, and  
11 this two-variable parameterization showed a superior performance to a parameterization based  
12 on CO<sub>2</sub><sup>+</sup> alone, because CO<sup>+</sup> and CO<sub>2</sub><sup>+</sup> show different seasonal trends.

13 PMF analysis was conducted on both the offline-AMS data described above and a set of  
14 molecular markers together with total OM. Biomass burning was found to be the largest OM  
15 source in winter, while secondary OA was largest in summer. However, higher concentrations  
16 of primary anthropogenic sources (traffic and biomass burning) were found at the urban  
17 background station of Vilnius. The offline-AMS and marker-based analyses also identified  
18 local emissions and primary biological particles, respectively, as factors with low overall but  
19 episodically important contributions to PM. Both methods showed traffic exhaust emissions  
20 to be only minor contributors to the total OM; which is not surprising given the distance of  
21 the three sampling stations from busy roads.

22 The two PMF analyses apportioned SOA to sources in different ways. The offline-AMS data  
23 yielded factors related to regional background (B-OOA) and temperature-driven (likely  
24 biogenic-influenced) emissions (S-OOA), while the marker-PMF yielded factors related to  
25 nitrate, sulfate, and MSA. For the offline-AMS PMF, S-OOA was the dominant factor in  
26 summer and showed a positive exponential correlation with the average daily temperature,  
27 similar to the behavior observed by Leaitch et al. (2011) in a Canadian boreal forest.  
28 Combining the two source apportionment techniques suggests that the S-OOA factor includes  
29 contributions from both terrestrial and marine secondary biogenic sources, while only small  
30 PBOA contributions to submicron OOA factors are possible. The analysis highlights the  
31 importance of regional meteorological conditions on air pollution in the southeastern Baltic  
32 region, as evidenced by simultaneous high BBOA levels at the three stations during three





1 different episodes in winter and by statistically similar S-OOA concentrations across the three  
2 stations during summer.

3

#### 4 **Acknowledgements**

5 The research leading to these results received funding from the Lithuanian–Swiss  
6 Cooperation Programme “Research and Development” project AEROLIT (Nr. CH-3-ŠMM-  
7 01/08). JGS acknowledges the support of the Swiss National Science Foundation (Starting  
8 Grant No. BSSGI0 155846). IE-H acknowledges the support of the Swiss National Science  
9 Foundation (IZERZO 142146).

10



1 References

- 2 Aiken, A. C., DeCarlo, P. F., Kroll, J. H., Worsnop, D. R., Huffman, J. A., Docherty, K. S.,  
3 Ulbrich, I. M., Mohr, C., Kimmel, J. R., Sueper, D., Sun, Y., Zhang, Q., Trimborn, A.,  
4 Northway, M., Ziemann, P. J., Canagaratna, M. R., Onasch, T. B., Alfarra, M. R., Prevot, A.  
5 S. H., Dommen, J., Duplissy, J., Metzger, A., Baltensperger, U., and Jimenez J. L. O/C and  
6 OM:OC ratios of primary, secondary, and ambient organic aerosols with high-resolution time-  
7 of-flight aerosol mass spectrometry. *Environ. Sci. Technol.* 42, 4478-4485, 2008.
- 8 Aksoyoglu, S., Keller, J., Barmadimos, I., Oderbolz, D., Lanz, V. A., Prévôt, A. S. H., and  
9 Baltensperger U.: Aerosol modelling in Europe with a focus on Switzerland during summer  
10 and winter episodes, *Atmos. Chem. Phys.*, 11, 7355–7373, 2011.
- 11 Aksoyoglu, S., Keller, J., Ciarelli, G., Prévôt, A. S. H., and Baltensperger, U.: A model study  
12 on changes of European and Swiss particulate matter, ozone and nitrogen deposition between  
13 1990 and 2020 due to the revised Gothenburg protocol, *Atmos. Chem. Phys.*, 14, 13081-  
14 13095, doi:10.5194/acp-14-13081-2014, 2014.
- 15 Alfarra, M. R., Prévôt, A. S. H., Szidat, S., Sandradewi, J., Weimer, S., Lanz, V. A.,  
16 Schreiber, D., Mohr, M., and Baltensperger, U.: Identification of the mass spectral signature  
17 of organic aerosols from wood burning emissions, *Environ. Sci. Technol.*, 41, 5770–5777,  
18 2007.
- 19 Allan, J. D., Delia, A. E., Coe, H., Bower, K. N., Alfarra, M. R., Jimenez, J. L., Middlebrook,  
20 A. M., Drewnick, F., Onasch, T. B., and Canagaratna, M. R.: A generalized method for the  
21 extraction of chemically resolved mass spectra from Aerodyne aerosol mass spectrometer  
22 data, *J. Aerosol Sci.* 35, 909-922, 2004.
- 23 Allan, J. D., Jimenez, J. L., Williams, P. I., Alfarra, M. R., Bower, K. N., Jayne, J. T., Coe,  
24 H., and Worsnop, D. R.: Quantitative sampling using an Aerodyne aerosol mass spectrometer:  
25 I. Techniques of data interpretation and error analysis, *J. Geophys. Res.-Atmos.*, 108, 4090,  
26 2003.
- 27 Baklanov, A., Schlünzen, K., Suppan, P., Baldasano, J., Brunner, D., Aksoyoglu, S.,  
28 Carmichael, G., Douros, J., Flemming, J., Forkel, R., Galmarini, S., Gauss, M., Grell, G.,  
29 Hirtl, M., Joffre, S., Jorba, O., Kaas, E., Kaasik, M., Kallos, G., Kong, X., Korsholm, U.,  
30 Kurganskiy, A., Kushta, J., Lohmann, U., Mahura, A., Manders-Groot, A., Maurizi, A.,  
31 Moussiopoulos, N., Rao, S. T., Savage, N., Seigneur, C., Sokhi, R. S., Solazzo, E.,



- 1 Solomos, S., Sørensen, B., Tsegas, G., Vignati, E., Vogel, B., and Zhang, Y.: Online coupled  
2 regional meteorology chemistry models in Europe: current status and prospects, Atmos.  
3 Chem. Phys., 14, 317-398, doi:10.5194/acp-14-317-2014, 2014.
- 4 Besombes, J.-L., Maître, A., Patissier, O., Marchand, N., Chevron, N., Stoklov, M., Masclet,  
5 P.: Particulate PAHs observed in the surrounding of a municipal incinerator.  
6 Atmos. Environ. 35, 6093–6104, 2001.
- 7 Birch, M. E. and Cary, R. A.: Elemental carbon-based method for monitoring occupational  
8 exposures to particulate diesel exhaust, Aerosol Sci. and Tech., 25, 221–241, 1996.
- 9 Bozzetti, C., Daellenbach, K., R., Hueglin, C., Fermo, P., Sciare, J., Kasper-Giebl, A., Mazar,  
10 Y., Abbaszade, G., El Kazzi, M., Gonzalez, R., Shuster Meiseles, T., Flasch, M., Wolf, R.,  
11 Křepelová, A., Canonaco, F., Schnelle-Kreis, J., Slowik, J. G., Zimmermann, R., Rudich, Y.,  
12 Baltensperger, U., El Haddad, I., and Prévôt, A. S. H.: Size-Resolved Identification,  
13 Characterization, and Quantification of Primary Biological Organic Aerosol at a European  
14 Rural Site, Environ. Sci. Technol., doi: 10.1021/acs.est.5b05960, 2016.
- 15 Bressi, M., Sciare, J., Gherzi, V., Mihalopoulos, N., Petit, J.-E., Nicolas, J. B., Moukhtar, S.,  
16 Rosso, A., Féron, A., Bonnaire, N., Poulakis, E., and Theodosi, C.: Sources and geographical  
17 origins of fine aerosols in Paris (France), Atmos. Chem. Phys., 14, 8813–8839, 2014.
- 18 Brown, S. G., Eberly, S., Paatero, P., and Norris, G. A., Methods for estimating uncertainty in  
19 PMF solutions: Examples with ambient air and water quality data and guidance on reporting  
20 PMF results, Sci. Tot. Environ. 518-519, 626-635, 2015.
- 21 Bruns, E. A., Krapf, M., Orasche, J., Huang, Y., Zimmermann, R., Drinovec, L., Močnik, G.,  
22 El-Haddad, I., Slowik, J. G., Dommen, J., Baltensperger, U. and Prévôt, A. S. H.:  
23 Characterization of primary and secondary wood combustion products generated under  
24 different burner loads, Atmos. Chem. Phys., 15, 2825–2841, 2015.
- 25 Byčenkienė, S., Ulevicius, V., Plauškaitė, K., Bozzetti, C., Fröhlich, R., Mordas, G., Slowik,  
26 J. G., El Haddad, I., Canonaco, F., and Prévôt A. S. H.: Source apportionment of the  
27 carbonaceous aerosols during wintertime over urban environment, *in prep.*
- 28 Canagaratna, M. R., Jayne, J. T., Jimenez, J. L., Allan, J. D., Alfarra, M. R., Zhang, Q.,  
29 Onasch, T. B., Drewnick, F., Coe, H., Middlebrook, A., Delia, A., Williams, L. R., Trimborn,  
30 A. M., Northway, M. J., DeCarlo, P. F., Kolb, C. E., Davidovits, P. and Worsnop, D. R.:



- 1 Chemical and microphysical characterization of ambient aerosols with the Aerodyne aerosol  
2 mass spectrometer, *Mass Spectrom. Rev.* 26:185-222, 2007.
- 3 Canagaratna, M. R., Jimenez, J. L., Kroll, J. H., Chen, Q., Kessler, S. H., Massoli, P.,  
4 Hildebrandt Ruiz, L., Fortner, E., Williams, L. R., Wilson, K. R., Surratt, J. D.,  
5 Donahue, N. M., Jayne, J. T., and Worsnop, D. R.: Elemental ratio measurements of organic  
6 compounds using aerosol mass spectrometry: characterization, improved calibration, and  
7 implications, *Atmos. Chem. Phys.*, 15, 253-272, doi:10.5194/acp-15-253-2015, 2015.
- 8 Canonaco, F., Crippa, M., Slowik, J. G., Baltensperger, U., and Prévôt, A. S. H.: SoFi, an  
9 IGOR-based interface for the efficient use of the generalized multilinear engine (ME-2) for  
10 the source apportionment: ME-2 application to aerosol mass spectrometer data, *Atmos. Meas.*  
11 *Tech.*, 6, 3649-3661, 2013.
- 12 Canonaco, F., Slowik, J. G., Baltensperger, U., and Prévôt, A. S. H.: Seasonal differences in  
13 oxygenated organic aerosol composition: implications for emissions sources and factor  
14 analysis. *Atmos. Chem. Phys.* 15, 6993-7002, 2015.
- 15 Cavalli, F., Viana, M., Yttri, K. E., Genberg, J., and Putaud, J. P.: Toward a standardised  
16 thermal-optical protocol for measuring atmospheric organic and elemental carbon: the  
17 EUSAAR protocol, *Atmos. Meas. Tech.*, 3, 79-89, 2010.
- 18 Chow, J., Watson, J., Ashbaugh, L. L., and Magliano, K. L.: Similarities and differences in  
19 PM10 chemical source profiles for geological dust from the San Joaquin Valley, California.  
20 *Atmos. Environ.* 37, 1317-1340, 2003.
- 21 Crippa, M., Canonaco, F., Lanz, V. A., Äijälä, M., Allan, J. D., Carbone, S., Capes, G.,  
22 Ceburnis, D., Dall'Osto, M., Day, D. A., DeCarlo, P. F., Ehn, M., Eriksson, A., Freney, E.,  
23 Hildebrandt Ruiz, L., Hillamo, R., Jimenez, J. L., Junninen, H., Kiendler-Scharr, A.,  
24 Kortelainen, A. M., Kulmala, M., Laaksonen, A., Mensah, A. A., Mohr, C., Nemitz, E.,  
25 O'Dowd, C., Ovadnevaite, J., Pandis, S. N., Petäjä, T., Poulain, L., Saarikoski, S., Sellegri, K.,  
26 Swietlicki, E., Tiitta, P., Worsnop, D. R., Baltensperger, U., and Prévôt, A. S. H.: Organic  
27 aerosol components derived from 25 AMS data sets across Europe using a consistent ME-2  
28 based source apportionment approach, *Atmos. Chem. Phys.*, 14, 6159–6176, 2014.
- 29 Crippa, M., El Haddad, I., Slowik, J. G., DeCarlo, P.F., Mohr, C., Heringa, M. F., Chirico, R.,  
30 Marchand, N., L., Sciare, J., Baltensperger, U., and Prévôt, A. S. H.: Identification of marine



- 1 and continental aerosol sources in Paris using high resolution aerosol mass spectrometry, J.  
2 Geophys. Res., 118, 1950-1963, 2013.
- 3 Daellenbach, K. R., Bozzetti, C., Krepelova, A., Canonaco, F., Huang, R.-J., Wolf, R., Zotter,  
4 P., Crippa, M., Slowik, J., Zhang, Y., Szidat, S., Baltensperger, U., Prévôt, A. S. H., and El  
5 Haddad, I.: Characterization and source apportionment of organic aerosol using offline  
6 aerosol mass spectrometry, Atmos. Meas. Tech., 9, 23-39, 2016.
- 7 Davison, A. C. and Hinkley, D. V.: Bootstrap Methods and Their Application, Cambridge  
8 University Press, Cambridge, UK, 582 pp., 1997.
- 9 DeCarlo, P. F., Kimmel, J. R., Trimborn, A., Northway, M. J., Jayne, J. T., Aiken, A. C.,  
10 Gonin, M., Fuhrer, K., Horvath, T., Docherty, K. S., Worsnop, D. R., and Jimenez, J. L.:  
11 Field-deployable, high-resolution, time-of-flight aerosol mass spectrometer, Anal. Chem., 78,  
12 8281–8289, 2006.
- 13 Dockery, D. W., Luttmann-Gibson, H., Rich, D. Q., Link, M. S., Mittleman, M. A., Gold, D.  
14 R., Koutrakis, P., Schwartz, J. D., and Verrier, R. L.: Association of air pollution with  
15 increased incidence of ventricular tachyarrhythmias recorded by implanted cardioverter  
16 defibrillators, Environ. Health Perspect. 113:670-674, 2005.
- 17 Docherty, K. S., Aiken, A. C., Huffman, J. A., Ulbrich, I. M., DeCarlo, P. F., Sueper, D.,  
18 Worsnop, D. R., Snyder, D. C., Peltier, R. E., Weber, R. J., Grover, B. D., Eatough, D. J.,  
19 Williams, B. J., Goldstein, A. H., Ziemann, P. J., and Jimenez, J. L.: The 2005 Study of  
20 Organic Aerosols at Riverside (SOAR-1): instrumental intercomparisons and fine particle  
21 composition, Atmos. Chem. Phys., 11, 12387-12420, doi:10.5194/acp-11-12387-2011, 2011.
- 22 Dudoitis, V., Byčenkienė, S., Plauškaitė, K., Bozzetti, C., Fröhlich, R., Mordas, G., and  
23 Ulevicius V.: Spatial distribution of carbonaceous aerosol in the southeastern Baltic region  
24 (event of grass fires), Acta Geophys., *in press*, 2015.
- 25 El Haddad, I., D'Anna, B., Temime-Roussel, B., Nicolas, M., Boreave, A., Favez, O., Voisin,  
26 D., Sciare, J., George, C., Jaffrezo, J.-L., Wortham, H., and Marchand, N.: Towards a better  
27 understanding of the origins, chemical composition and aging of oxygenated organic aerosols:  
28 case study of a Mediterranean industrialized environment, Marseille, Atmos. Chem. Phys., 13,  
29 7875-7894, doi:10.5194/acp-13-7875-2013, 2013.
- 30 El Haddad, I., Marchand, N., Dron, J., Temime-Roussel, B., Quivet, E., Wortham, H.,  
31 Jaffrezo, J. L., Baduel, C., Voisin, D., Besombes, J. L., and Gille, G.: Comprehensive primary



- 1 particulate organic characterization of vehicular exhaust emissions in France, Atmos.  
2 Environ., 43, 6190–6198, 2009.
- 3 Elser, M., Bozzetti, C., El-Haddad, I., Maasikmets, M., Teinmaa, E., Richter, R., Wolf, R.,  
4 Slowik, J. G., Baltensperger, U., and Prévôt, A. S. H.: Urban increments of gaseous and  
5 aerosol pollutants and their sources using mobile aerosol mass spectrometry measurements,  
6 Atmos. Chem. Phys. Discuss., doi:10.5194/acp-2016-31, 2016.
- 7 Elser, M., Huang, R.-J., Wolf, R., Slowik, J. G., Wang, Q., Canonaco, F., Li, G., Bozzetti, C.,  
8 Daellenbach, K. R., Huang, Y., Zhang, R., Li, Z., Cao, J., Baltensperger, U., El-Haddad, I.,  
9 and Prévôt, A. S. H.: New insights into PM<sub>2.5</sub> chemical composition and sources in two  
10 major cities in China during extreme haze events using aerosol mass spectrometry, Atmos.  
11 Chem. Phys., 16, 3207-3225, doi:10.5194/acp-16-3207-2016, 2016.
- 12 Fraser, M. P., Cass, G. R., and Simoneit, B. R. T.: Gas-phase and particle-phase organic  
13 compounds emitted from motor vehicle traffic in a Los Angeles roadway tunnel, Environ. Sci.  
14 Technol. 14, 2051-2060, 1998.
- 15 Fröhlich, R., Cubison, M. J., Slowik, J. G., Bukowiecki, N., Prevot, A. S. H., Baltensperger,  
16 U., Schneider, J., Kimmel, J. R., Gonin, M., Rohner, U., Worsnop, D. R. and Jayne J. T.: The  
17 ToF-ACSM: a portable aerosol chemical speciation monitor with TOFMS detection, Atmos.  
18 Meas. Tech., 6, 3225-3241, 2013.
- 19 Golly, B., Brulfert, G., Berlioux G., Jaffrezo J.-L., Besombes, J.-L.: Large chemical  
20 characterisation of PM<sub>10</sub> emitted from graphite material production: Application in source  
21 apportionment, Sci. Tot. Environ., 538, 634–643, 2015.
- 22 Guenther, A., Karl, T., Harley, P., Wiedinmyer, C., Palmer, P. I., and Geron, C.: Estimates of  
23 global terrestrial isoprene emissions using MEGAN (Model of Emissions of Gases and  
24 Aerosols from Nature), Atmos. Chem. Phys., 6, 3181-3210, doi:10.5194/acp-6-3181-2006,  
25 2006.
- 26 He, L.-Y., Hu, M., Zhang, Y.-H., Huang, X.-F. and Yao, T.-T: Chemical characterization of  
27 fine particles from on-road vehicles in the Wutong tunnel in Shenzhen, China, Chemosphere  
28 62, 1565-1573, 2006.
- 29 He, L.-Y., Hu, M., Zhang, Y.-H., Huang, X.-F., and Yao, T.-T. Fine particle emissions from  
30 onroad vehicles in the Zhujiang tunnel, China, Environ. Sci. Technol., 42, 4461-4466, 2008.



- 1 Herich, H., Gianini, M. F. D., Piot, C., Močnik, G., Jaffrezo, J. L., Besombes, J. L., Prévôt, A.  
2 S. H., and Hueglin, C.: Overview of the impact of wood burning emissions on carbonaceous  
3 aerosols and PM in large parts of the Alpine region, *Atmos. Environ.*, 89, 64–75,  
4 doi:10.1016/j.atmosenv.2014.02.008, 2014.
- 5 Huang, R.-J., Zhang, Y., Bozzetti, C., Ho, K.-F., Cao, J., Han, Y., Dällenbach, K. R., Slowik,  
6 J. G., Platt, S. M., Canonaco, F., Zotter, P., Wolf, R., Pieber, S. M., Bruns, E. A., Crippa, M.,  
7 Ciarelli, G., Piazzalunga, A., Schwikowski, M., Abbaszade, G., Schnelle-Kreis, J.,  
8 Zimmermann, R., An, Z., Szidat, S., Baltensperger, U., Haddad, I. E., and Prévôt, A. S. H.:  
9 High secondary aerosol contribution to particulate pollution during haze events in China,  
10 *Nature*, 514, 2014.
- 11 Jaffrezo, J.-L., Aymoz, G., Delaval, C., and Cozic J.: Seasonal evolution of the soluble  
12 fraction of particulate organic carbon in Alpine Valleys. *Atmos. Chem. Phys.*, 5, 2809–2821,  
13 2005.
- 14 Jaffrezo, J. L., Calas, T., and Bouchet, M.: Carboxylic acids measurements with ionic  
15 chromatography, *Atmos. Environ.*, 32, 2705–2708, 1998.
- 16 Jardine, K., Yañez-Serrano, A. M., Williams, J., Kunert, N., Jardine, A., Taylor, T., Abrell,  
17 L., Artaxo, P., Guenther, A., Hewitt, C. N., House, E., Florentino, A. P., Manzi, A., Higuchi,  
18 N., Kesselmeier, J., Behrendt, T, Veres, P. R., Derstroff, B., Fuentes, J. D., Martin, S. T., and  
19 Andreae, M. O.: Dimethyl Sulfide in the Amazon Rain Forest, *Global Biogeochem. Cy.*, 29,  
20 19–32, 2015.
- 21 Klein, F., Platt, S. M., Farren, N. J., Detournay, A., Bruns, E. A., Bozzetti, C., Daellenbach,  
22 K. R., Kilic, D., Kumar, N. K., Pieber, S. M., Slowik, J. G., Temime-Roussel, B., Marchand,  
23 N., Hamilton, J. F., Baltensperger, U., Prévôt, A. S. H., and El Haddad, I.: Characterization of  
24 gas-phase organics using proton transfer reaction time-of-flight mass spectrometry: cooking  
25 emissions, *Environ. Sci. Technol.*, 50, 1243–1250, 2016.
- 26 Laden, F., Neas, L. M., Dockery, D. W., and Schwartz, J.: Association of fine particulate  
27 matter from different sources with daily mortality in six US cities, *Environ. Health Perspect.*  
28 108:941–947, 2000.
- 29 Lanz, V. A., Alfarra, M. R., Baltensperger, U., Buchmann, B., Hueglin, C., and Prévôt, A. S.  
30 H.: Source apportionment of submicron organic aerosols at an urban site by factor analytical



- 1 modelling of aerosol mass spectra, *Atmos. Chem. Phys.*, 7, 1503-1522, doi:10.5194/acp-7-  
2 1503-2007, 2007.
- 3 Lanz, V. A., Prévôt, A. S. H., Alfarra, M. R., Weimer, S., Mohr, C., DeCarlo, P. F., Gianini,  
4 M. F. D., Hueglin, C., Schneider, J., Favez, O., D'Anna, B., George, C., and  
5 Baltensperger, U.: Characterization of aerosol chemical composition with aerosol mass  
6 spectrometry in Central Europe: an overview, *Atmos. Chem. Phys.*, 10, 10453–10471, 2010.
- 7 Leaitch, W. R. Macdonald, A. M., Brickell, P. C., Liggio, J., Sjostedt, S. J., Vlasenko, A.,  
8 Bottenheim, J. W., Huang, L., Li, S.-M., Liu, P. S. K., Toom-Sauntry, D., Hayden, K. A.,  
9 Sharma, S., Shantz, N. C., Wiebe H. A., Zhang, W., Abbatt, J. P. D., Slowik, J. G., Chang,  
10 Rachel, Y.-W., Russell, L. M., Schwartz, R. E., Takahama, S., Jayne, J. T., Ng, N. L.:  
11 Temperature response of the submicron organic aerosol from temperate forests, *Atmos.*  
12 *Environ.*, 45, 6696-6704, 2011.
- 13 Lee, A. K. Y., Herckes, P., Leaitch, W. R., Macdonald, A. M., and Abbatt, J. P. D.: Aqueous  
14 OH oxidation of ambient organic aerosol and cloud water organics: Formation of highly  
15 oxidized products, *Geoph. Res. Lett.*, 38, L11 805, 2011.
- 16 Li, S.M., Talbot, R.W., Barrie, L.A., Harriss, R.C., Davidson, C.I. and Jaffrezo, J.-L.:  
17 Seasonal and geographic variations of methanesulfonic acid in the Arctic troposphere, *Atmos.*  
18 *Environ.*, 27A, 3011-3024, 1993.
- 19 Lohmann, U., Broekhuizen, K., Leaitch, R., Shantz, N., and Abbatt, J.: How efficient is cloud  
20 droplet formation of organic aerosols?, *Geophys. Res. Lett.* 31, L05108, 2004.
- 21 Manish K. S., Subramanian, R., Rogge, W. F., and Robinson, A. L.: Sources of organic  
22 aerosol: Positive matrix factorization of molecular marker data and comparison of results  
23 from different source apportionment models, *Atmos. Environ.*, 41, 9353-9369, 2007.
- 24 Mihara, T. and Mochida, M.: Characterization of solvent-extractable organics in urban  
25 aerosols based on mass spectrum analysis and hygroscopic growth measurement, *Envir. Sci.*  
26 *Tech.*, 45, 9168–9174, 2011.
- 27 Minguillón, M. C., Perron, N., Querol, X., Szidat, S., Fahrni, S. M., Alastuey, A., Jimenez, J.  
28 L., Mohr, C., Ortega, A. M., Day, D. A., Lanz, V. A., Wacker, L., Reche, C., Cusack, M.,  
29 Amato, F., Kiss, G., Hoffer, A., Decesari, S., Moretti, F., Hillamo, R., Teinila, K., Seco, R.,  
30 Penuelas, J., Metzger, A., Schallhart, S., Muller, M., Hansel, A., Burkhardt, J. F.,  
31 Baltensperger, U., and Prevot, A. S. H.: Fossil versus contemporary sources of fine elemental





- 1 and organic carbonaceous particulate matter during the DAURE campaign in Northeast Spain,  
2 Atmos. Chem. Phys., 11, 12067-12084, 2011.
- 3 Mohr, C., DeCarlo, P. F., Heringa, M. F., Chirico, R., Slowik, J. G., Richter, R., Reche, C.,  
4 Alastuey, A., Querol, X., Seco, R., Penuelas, J., Jimenez, J. L., Crippa, M., Zimmermann, R.,  
5 Baltensperger, U., and Prevot, A. S. H.: Identification and quantification of organic aerosol  
6 from cooking and other sources in Barcelona using aerosol mass spectrometer data, Atmos.  
7 Chem. Phys., 12, 1649-1665, 2012.
- 8 Mordas, G., Plauškaitė, K., Prokopčiuk, N., Dudoitis, V., Bozzetti, C. and Ulevicius, V.:  
9 Observation of new particle formation on Curonian Spit located between continental Europe  
10 and Scandinavia, J Aerosol Sci, 97, 38-55, 2016.
- 11 Ng, N. L., Herndon, S. C., Trimborn, A., Canagaratna, M. R., Croteau, P. L., Onasch, T. B.  
12 Sueper, D., Worsnop, D. R., Zhang, Q., Sun, Y. L. and Jayne, J. T.: An Aerosol Chemical  
13 Speciation Monitor (ACSM) for routine monitoring of the composition and mass  
14 concentrations of ambient aerosol, Aerosol Sci. Tech., 45, 770-784, 2011.
- 15 Paatero, P.: Least squares formulation of robust non-negative factor analysis, Chemom. Intell.  
16 Lab. Syst., 37, 23–35, 1997.
- 17 Paatero, P.: The multilinear engine - A table-driven, least squares program for solving  
18 multilinear problems, including the n-way parallel factor analysis model, J. Comput. Graph.  
19 Stat., 8, 854-888, 1999.
- 20 Paatero, P. and Tapper, U.: Positive matrix factorization - a nonnegative factor model with  
21 optimal utilization of error-estimates of data values, Environmetrics, 5, 111-126, 1994.
- 22 Rocke, D. M., and Lorenzato, S.: A two-component model for measurement error in  
23 analytical chemistry, Technometrics, 37, 176-184, 1995.
- 24 Rutter, A. P., Snyder, D. C., Schauer, J. J., DeMinter, J. and Shelton, B.: Sensitivity and bias  
25 of molecular marker-based aerosol source apportionment models to small contributions of  
26 coal combustion soot, Environ. Sci. Technol., 43, 7770-7777, 2009.
- 27 Schauer, J. J., Kleeman, M. J., Cass, G. R., and Simoneit, B. T.: Measurement of emissions  
28 from air pollution sources. 3. C1-C29 organic compounds from fireplace combustion of  
29 wood, Environ. Sci. Technol., 35, 1716-1728, 2001.



- 1 Schwarze, P. E., Ovrevik, J., Lag, M., Refsnes, M., Nafstad, P., Hetland, R. B., and Dybing,  
2 E.: Particulate matter properties and health effects: consistency of epidemiological and  
3 toxicological studies, *Hum. Exp. Toxicol.* 25, 559-579, 2006.
- 4 Setyan, A., Zhang, Q., Merkel, M., Knighton, W. B., Sun, Y., Song, C., Shilling, J. E.,  
5 Onasch, T. B., Herndon, S. C., Worsnop, D. R., Fast, J. D., Zaveri, R. A., Berg, L. K.,  
6 Wiedensohler, A., Flowers, B. A., Dubey, M. K., and Subramanian R.: Characterization of  
7 submicron particles influenced by mixed biogenic and anthropogenic emissions using high-  
8 resolution aerosol mass spectrometry: results from CARES, *Atmos. Chem. Phys.*, 12, 8131-  
9 8156, 2012.
- 10 Subramanian, R., Donahue, N. M., Bernardo-Bricker, A., Rogge, W. F., and Robinson, A. L.:  
11 Contribution of motor vehicle emissions to organic carbon and fine particle mass in  
12 Pittsburgh, Pennsylvania: Effects of varying source profiles and seasonal trends in ambient  
13 marker concentrations, *Atmos. Environ.*, 40, 8002-8019, 2006.
- 14 Subramanian, R., Donahue, N. M., Bernardo-Bricker, A., Rogge, W. F., and Robinson, A. L.:  
15 Insights into the primary-secondary and regional-local contributions to organic aerosol and  
16 PM<sub>2.5</sub> mass in Pittsburgh, Pennsylvania, *Atmos. Environ.*, 41, 7414-7433, 2007.
- 17 Sun, Y., Zhang, Q., Zheng, M., Ding, X., Edgerton, E. S., and Wang, X.: Characterization and  
18 source apportionment of water-soluble organic matter in atmospheric fine particles (PM<sub>2.5</sub>)  
19 with High-Resolution Aerosol Mass Spectrometry and GC-MS, *Envir. Sci. Tech.*, 45, 4854-  
20 4861, 2011.
- 21 Ulbrich, I. M., Canagaratna, M. R., Zhang, Q., Worsnop, D. R., and Jimenez, J. L.:  
22 Interpretation of organic components from positive matrix factorization of aerosol mass  
23 spectrometric data, *Atmos. Chem. Phys.*, 9, 2891-2918, 2009.
- 24 Ulevicius, V., Byčenkienė, S., Bozzetti, C., Vlachou, A., Plauškaitė, K., Mordas, G., Dudoitis,  
25 V., Abbaszade, G., Remeikis, V., Garbaras, A., Masalaite, A., Bles, J., Fröhlich, R.,  
26 Dällenbach, K. R., Canonaco, F., Slowik, J. G., Dommen, J., Zimmermann, R., Schnelle-  
27 Kreis, J., Salazar, G. A., Agrios, K., Szidat, S., El Haddad, I., and Prévôt, A. S. H.: Fossil and  
28 non-fossil source contributions to atmospheric carbonaceous aerosols during extreme spring  
29 grassland fires in Eastern Europe. *Atmos. Chem. Phys.*, 16, 5513-5529, 2016.
- 30 Viana, M., Kuhlbusch, T. A. J., Querol, X., Alastuey, A., Harrison, R. M., Hopke, P. K.,  
31 Winiwarter, W., Vallius, M., Szidat, S., Prévôt, A. S. H., Hueglin, C., Bloemen, H., Wählin,

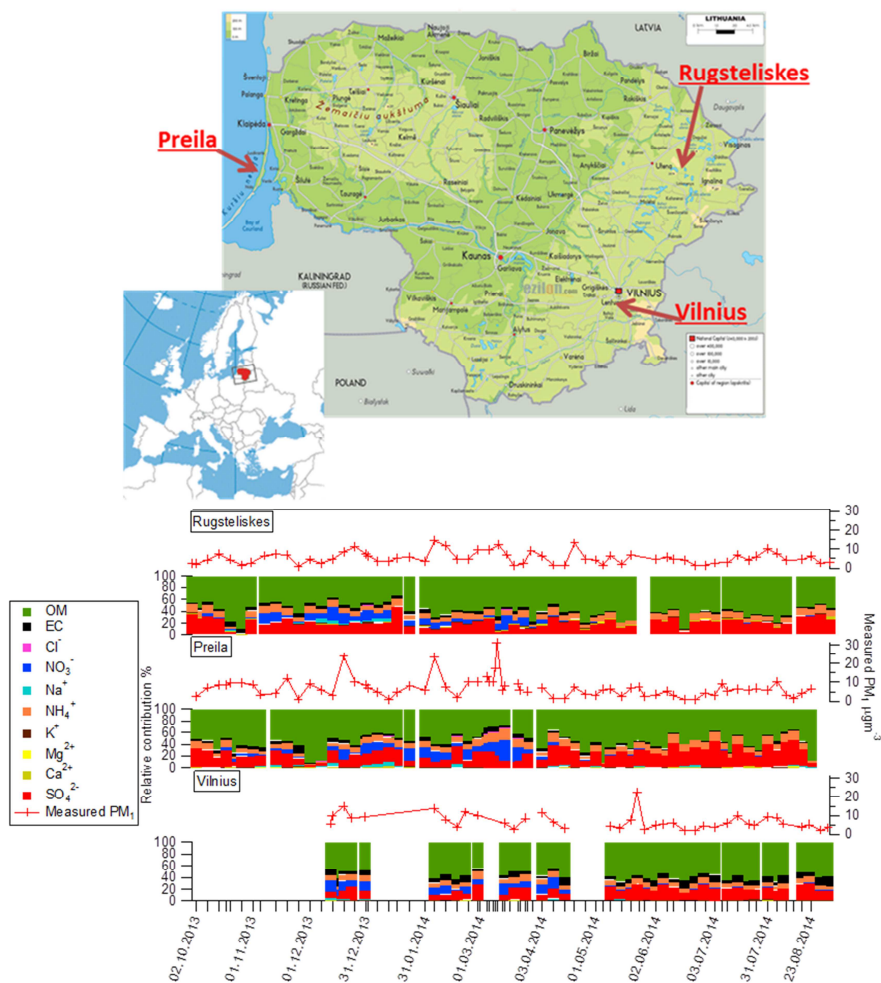


- 1 P., Vecchi, R., Miranda, A. I., Kasper-Giebl, A., Maenhaut, W., and Hitzenberger, R.: Source  
2 apportionment of particulate matter in Europe: a review of methods and results, *J. Aerosol*  
3 *Sci.*, 39, 827–849, doi:10.1016/j.jaerosci.2008.05.007, 2008.
- 4 Waked, A., Favez, O., Alleman, L. Y., Piot, C., Petit, J. E., Delaunay, T., Golly, B.,  
5 Besombes, J.-L., Jaffrezo, J.-L., and Leoz-Garziandia, E.: Source apportionment of PM10 in  
6 an urban site using a PMF model applied on inorganic and organic chemical species. *Atmos.*  
7 *Chem. Phys.*, 14, 3325-3346, 2014.
- 8 Zhang, Q., Jimenez, J. L., Canagaratna, M. R., Ulbrich, I. M., Ng, N. L., Worsnop, D. R., and  
9 Sun Y.: Understanding atmospheric organic aerosols via factor analysis of aerosol mass  
10 spectrometry: a review. *Anal Bioanal. Chem.*, 401, 3045-3067, 2011.
- 11 Zotter, P., Ciobanu, V. G., Zhang, Y. L., El Haddad, I., Macchia, M., Daellenbach, K. R.,  
12 Salazar, G. A., Huang, R.-J., Wacker, L., Hueglin, C., Piazzalunga, A., Fermo, P.,  
13 Schwikowski, M., Baltensperger, U., Szidat, S., and Prévôt, A. S. H.: Radiocarbon analysis of  
14 elemental and organic carbon in Switzerland during winter-smog episodes from 2008 to 2012  
15 – Part 1: Source apportionment and spatial variability, *Atmos. Chem. Phys.*, 14, 13551–  
16 13570, doi:10.5194/acp-14-13551-2014, 2014.

17

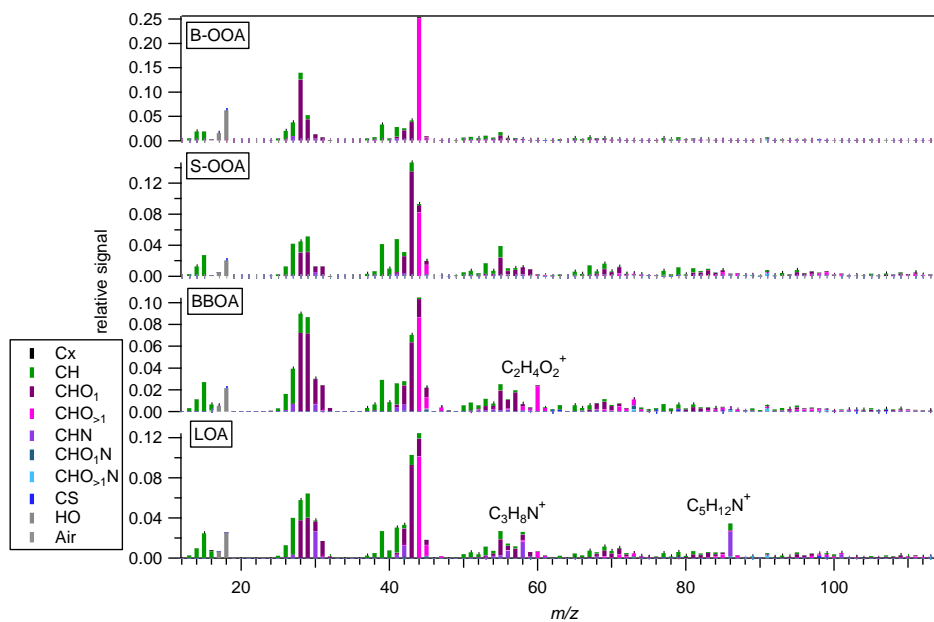


## 1 Figures main text



2

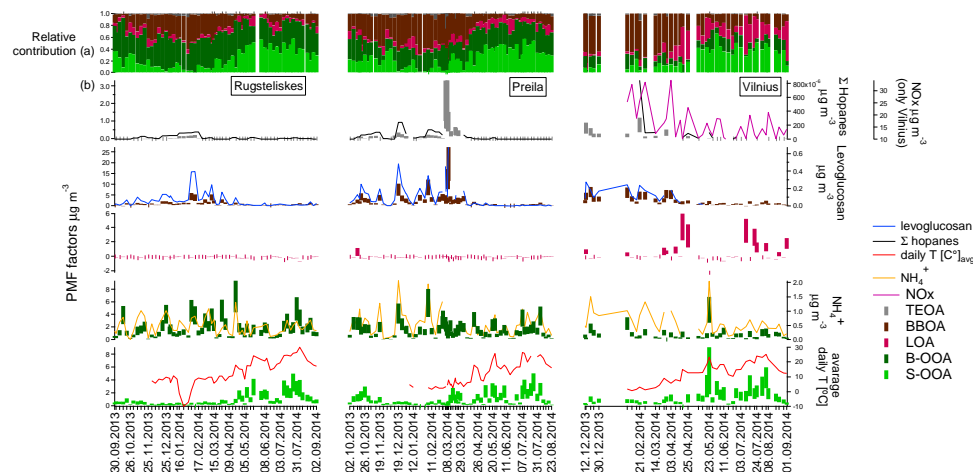
3 Figure 1. Sampling locations, and measured PM<sub>1</sub> composition.



1

2 Figure 2. Offline-AMS PMF factor profiles.

3

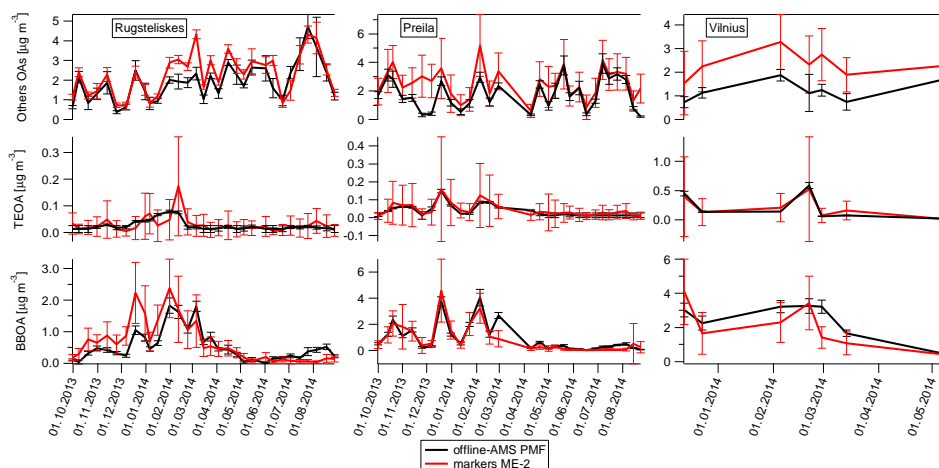


4

5 Figure 3. a) Temporal evolutions of relative contributions to the OA factors; b) OA sources  
 6 and corresponding tracers: concentrations and uncertainties (shaded areas).

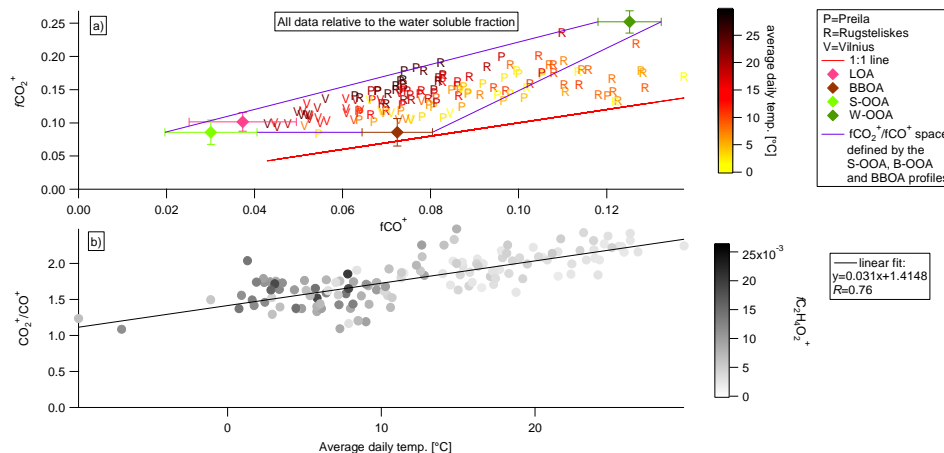
7





1

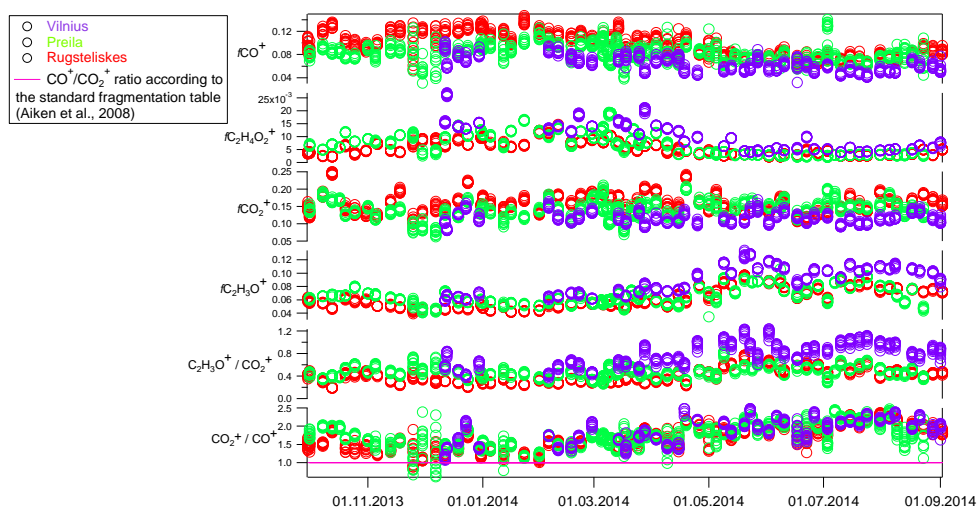
2 Figure 6. Marker-PMF and offline-AMS OM source apportionment comparison.



3

4 Figure 7. a) water-soluble  $f\text{CO}_2^+$  vs  $f\text{CO}^+$  scatter plot. Color code denotes the average daily  
 5 temperature [°C], diamonds indicate the  $f\text{CO}_2^+/f\text{CO}^+$  ratio for different PMF factor profiles.  
 6 The 1:1 line is displayed in red. Few points from Rūgštelīškis lie outside the triangle,  
 7 suggesting they are not well explained by our PMF model. However, Fig. S5 displays flat  
 8 residuals for Rūgštelīškis, indicating an overall good WSOM explained variability by the  
 9 model. b) Scatter plot of the water-soluble  $\text{CO}_2^+$  to  $\text{CO}^+$  ratio vs. average daily temperature.  
 10 Grey code denotes  $f\text{C}_2\text{H}_4\text{O}_2^+$ .

11



1

2 Figure 8. Time-dependent fractional contributions ( $f$ ) of typical AMS tracers.

3